High-strength wind turbine steel towers

Elforsk rapport: 09:11

Milan Veljkovic, Wylliam Husson Januari 2009

Vindforsk Energimyndigheten ELFORSK

High-strength wind turbine steel towers

Elforsk rapport: 09:11

Milan Veljkovic, Wylliam Husson

januari, 2009

Preface

This report is the final report for the the Vindfrosk project V-223 ”High strength steel tower sfor wind turbines. The project has been carried out within tha basic research part of the Vindforsk programme.

The project has been financed by Energimyndigheten as project P 31132-1.

The main objective of this project is to develop a new type of high steel towers that will lower the cost of wind turbine towers.

The project is a part of the EU HISTWIN project

The Vindforsk project has been carried out by Luleå University of Technology, Dept. of Civil, Mining and Environmental Engineering.

Comments on the work and the final report have been given by a reference group with the following members:

Sven-Erik Thor, Vattenfal Wind Power

Peter Overup och Mahyar Mansoori, EWP Windtower Production AB

Mats Wallin, DynaWind

Stockholm januari 2009

Anders Björck

Programme manager Vindforsk II

Sammanfattning

Rörformade ståltorn för vindkraftverk med multimegawatt-turbiner kan i dagsläget tillverkas med en navhöjd på upp till ca 100 m. Dessa är konformade med ökad diameter och plåttjocklek vid fundamentet.

Tornen består av 2-3 sektioner som tillverkas i verkstäder och därefter monteras ihop på byggarbetsplatsen. Restriktioner avseende transporter medför begränsningar på sektionernas diameter, längd och vikt. Vanligen begränsas diametern till ca 4.3 m, vikten till ca 60 ton och sektionernas längd till ca 25 m.

Ståltornen står för ca 15 till 20 % av den totala investeringskostnaden. En optimal dimensionering av förbanden i skarven mellan sektionerna har en stor inverkan på totalkostnaden. Ett innovativt friktionsförband, öppna långa slitsade hål, och dess implementering på stålrören betraktas. Det innovativa förbandet har avsevärt förbättrat det konstruktiva beteendet vid utmattningsbelastning, med minst dubbla utmattningskapaciteten och nästan inga begränsningar i förbandets hållfasthet. Detta möjliggör en optimering av tornets design och ett billigare in-situ montage. Dessutom öppnar friktionsförbandet nya möjligheter för vidare utveckling av konceptet med rörformade torn för högre tornhöjder.

Statiska och långtidsbelastade friktionsförband undersöks experimentellt och numeriskt. Dessa undersökningar har lett till nya rekommendationer för dimensionering som överensstämmer med befintliga dimensioneringsprinciper i Eurokoder samt Riktlinjer för certifiering av vindkraftverk som publicerats av Germanischer Lloyd WindEnergie.

Dimensioneringsexempel med det innovativa förbandet har gjorts och dessa jämförs med flänsförbandet i rapporten. Besparingen, endast baserad på minskad materialkostnad för förbanden, är minst 20000 Euro per vindkraftverk. Potentialen med större kostnadsfördelar finns i enklare och snabbare tornproduktion och in-situ montage, samt i optimering av dörröppningar. Dessa tilläggsfördelar har endast utvärderats kvantitativt, baserat på övervägandet av stål med hållfastheten större än S355 (sträckgränsen 355 MPa) vilket används som den högsta stålkvaliteten i tornen.

Arbetet som utförts vid Luleå tekniska universitet och övriga partners i det internationella projektet HISTWIN, skapar möjligheter att konstruera ett pilottorn med ”HISTWIN” (friktions-) förband.

Summary

Tubular steel towers for multi-megawatt turbines are currently available with hub height up to about 100 m. They have a slightly conical shape with increased diameter and plate thickness at the base.

The towers are made of 2-3 segments manufactured in a workshop and assembled on site. Transportation constraints impose limits on the diameter, length and weight of segments. Typically the diameter is limited to about 4.3 m, the mass about 60 tones and the segment length about 25 m.

The steel towers represent about 15 to 20% of the total installation costs. The optimal design of connection of the tower's segments have strong influence on the total price. An innovative friction type connection, open long slotted holes, and its implementation in the tubular towers are considered. The innovative connection has substantially improved structural performance of the connection in fatigue, at least double fatigue endurance and almost no limits to the connection strength. The enables optimization of the tower design and less expensive in-situ assembling. In addition the friction connection open possibilities for further development of the tubular tower concept.

The static and long term behaviours of flat segments are investigated experimentally and numerically. These investigations led to new design recommendations which comply with existing Eurocode design rules and Guidelines for the certification of Wind Turbines published by the Germanischer Lloyd WindEnergie.

Design examples of the innovative connection is prepared and savings, based only on reduced material costs of connections, are at least of 20000 Euros per tower is shown. The potential of having higher cost benefits are further influenced by easier and faster tower production and in-situ assembling, and by optimization of the door openings. These further benefits are only quantitatively assessed based on consideration of higher strength steel than S 355 (yield strength 355 MPa) which is used as the highest steel grade in the towers.

The work performed at Luleå University of Technology and other partners of international project HISTWIN, creates opportunities to design a pilot tower with "HISTWIN" (friction) connection.

Contents

1 Background

The project High-strength steel tower (2008-01-01-2008-12-31) granted by Energimyndigheten, Projeknr. 31132-1 to Luleå University of Technology (LTU), Dept. of Civil, Mining and Environmental Engineering, is part of the 3-years European project, HISTWIN, High-Strength Steel Tower for Wind Turbines, RFS-CT 2006-00031.

The total HISTWIN budget is 1.393.722 Euro, and total LTU:s budget is 320.962 Euro. The budget for LTU in 2008 was 1.495.000 sek including contribution from Energimyndigheten of 583 050 sek.

Following are HISTWIN project partners:

- Luleå University of Technology, Division of Steel Structures, Sweden (LTU), coordinator.
- Rheinisch Westfälische Technische Hochschule, Lehrstuhl für Stahlbau, Aachen, Germany (RWTH).
- Germanischer Lloyd Industrial Services GmbH, Germany (GL-WIND).
- Aristotle University of Thessaloniki - Institute of Steel Structures, Greece (AUTH).
- Repower Portugal Equipamentos Eólicos SA, Portugal (REPOWER).
- University of Coimbra, Faculty of Science and Technology, Department of Civil Engineering, Portugal (FCTUC).
- Rautaruukki Oyj, Finland (RUUKKI).

The aim of the HISTWIN project is to optimize the tower geometry and introduce innovative solutions for assembly joints.

The work planned for 2008, which is partially financed by Energimyndigheten, has the aim to:

- Evaluate existing design recommendations and propose a new solution for assembling joints.
- Choose material and design a tower's in-situ connections (assembling connections). Perform experiments necessary for structural properties of a new friction assembling connection and its evaluation. Finite element analysis of static experiments.
- Propose a new design recommendation, especially for the assembling joints.
- Examinate one Civil engineer, a diploma work, and one PhD student at licentiate level.

- Publish project results at two international conferences and present them to Technical Committee for Structural Connections, TC10 of ECCS.

The project "High-Strength Tower" is realized in four consecutive steps:

1 Experimental and numerical evaluation of a new assembling joint using a special bolt type and open slotted holes. The overall idea of a newly proposed connection is shown in Figure 1-1. Experiments are performed on segments of the cylinder.

Figure 1-1. The existing and the new innovative solution considered in the project.

2 Evaluation of the production costs for the new type of joint. A case study considering an assembled joint with traditional L-flange and standard bolts, and the new joint type using Tension Control Bolts will provide an estimation of the economical savings.

3 Influence of the weather conditions on strain level changes in the pre-stressed bolts will be estimated in laboratory conditions varying the temperature between -20^0C and $+20^0$C [*]. Temperature variation is achieved in LTU's Cold-climate chamber.

4 Numerical analysis to optimise tower thickness and possible changes in the door opening detail. The analysis will be performed on a wind tower for which design load tables are available.

[*] In-situ short term measurement was originally proposed. It is concluded that relevant information may be obtained in the laboratory conditions.

2 A new connection type

The most common in-situ connection between towers segments is the bolted L-flange connection where pairs of rather thick steel flanges (even more than 200 mm) are welded on the inside of the tubes and bolted together with pre-tensioned high strength bolts.

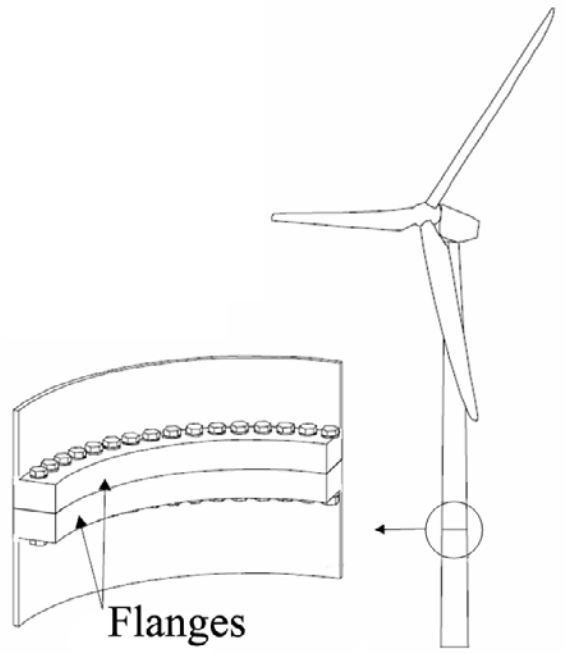

Figure 2-1. Bolted L-flange connection [1]**.**

The fabrication process is laborious and costly, and the design is based on complex models. The fatigue resistance is low, fatigue class between 36 to 71 [2] and can be the main design limitation. The fatigue class depends on fabrication process and connection detailing.

High Strength Friction Grip connections (or just friction connection) were shown to have a fatigue resistance similar or better than that of but welds, which means at least two times higher than the flange connection fatigue class [3, 4]. These joints also have higher stiffness [5] and good energy dissipation properties [6]. Their implementation in towers could thus shift the design limitations from joint to shell resistance and improve the overall structure efficiency.

High Strength Bolts of grade 10.9 placed in normal holes, i.e. with relatively low clearance are typically used in the friction connection. For practical and safety reasons the fasteners shall be tightened from within the tower only, and the holes shape and clearance shall be adapted to facilitate alignment of the sections and installation of the fasteners.

The principle of the considered solution is presented on Figure 2-2. Tension Control Bolts are used in long slotted holes.

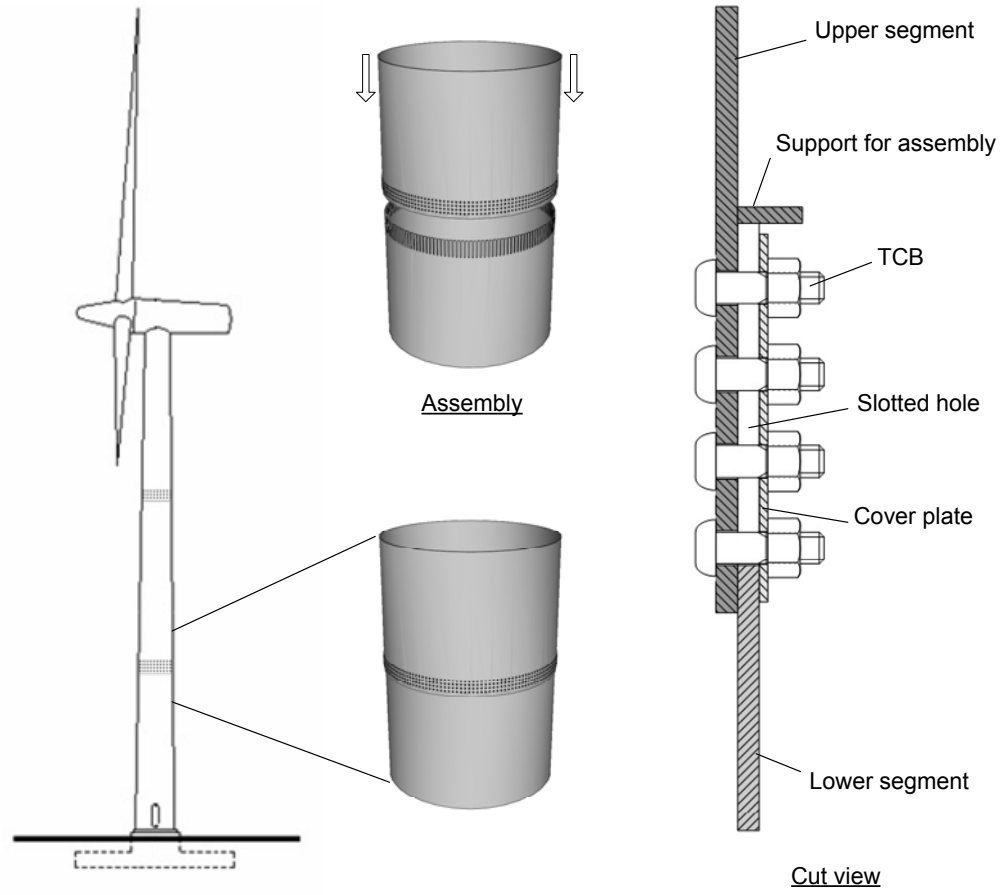

Figure 2-2. Principle of the proposed friction connection.

The lower segment has open slotted holes. The fasteners can be preinstalled in the normal holes of the upper segment and they can then be used for the angular alignment of the upper segment while it slides down in the position. Support must then be provided to hold the sections during tightening. Note here that the slots offer rather large flexibility in longitudinal tolerances. The reduced shell bending stiffness at the top of the lower segment allows rather big ovalness tolerance between two segments at the connection.

It was experimentally found that double lap joints using standard washers had relatively lower resistance with oversized holes [7] or slotted holes [8] compare to normal holes. This effect was related to the different contact distribution of higher contact pressure in the case of slotted holes [9]. A cover plate is used in the connections, see Figure 3-1, to remedy this problem.

The static behaviour and resistance as well as the long term behaviour thus need to be investigated for the new connection type.

Tension Control Bolts (TCBs) were considered as a possible fasteners because it was the only product available on the market that meets our requirements. They are a special type of high strength fasteners initially developed in Japan. Their tightening is carried out entirely at the nut end (See Figure 2-4) with a special electric wrench. The spline is held by the inner socket while the outer socket rotates and turns the nut (a). An increasing tightening torque develops between inner and outer socket. When the resistance of the calibrated break-neck is reached it shears off, allowing the inner socket to rotate (b).

This type of fasteners was chosen because it was available on the market and for its simple installation. The producer claims that tightening procedure can be up to two times quicker and requires four times less man hours than compared to normal bolts [10]. It might also be advantageous to rely on electrical power rather than pneumatic or hydraulic power which are more difficult to provide during assembly of a wind tower.

Moreover the mechanical properties are equivalent to those of High Strength Bolts; grade S10T may be considered as bolt grade 10.9 [11, 12].

Since tightening is performed at the nut end only, no torsion is introduced in the shank [10]. This property is believed to reduce the risk of self loosening.

The bolts from *Tension Control Bolts Ltd.* are also protected from corrosion with an environmental friendly Zn-Al polymetallic coating (*Greenkote*) that performs better than conventional coatings [10].

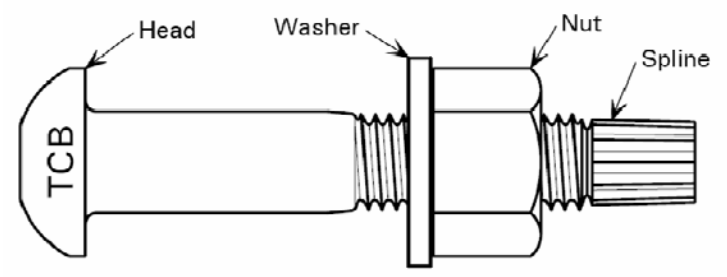

Figure 2-3. Tension Control Bolt, Grade S10T (Prior to pretensioning) [11]**.**

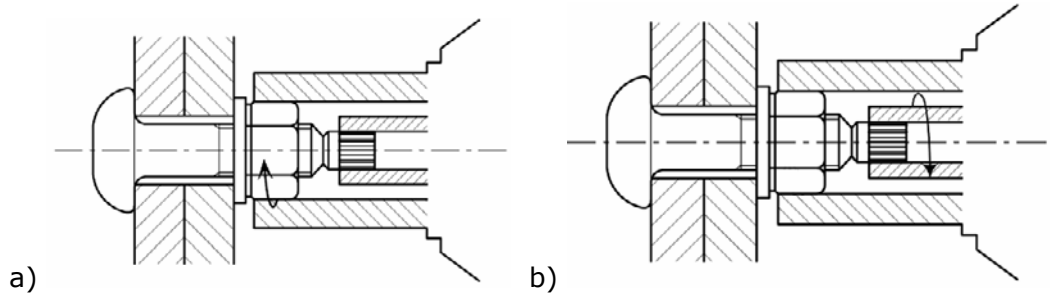

Figure 2-4. Tightening procedure; a) The outer socket turns the nut while the spline is held by the stationary inner socket; b) The tightening torque is sufficient to shear off the spline, allowing the inner socket to rotate. [11]

3 Static tests

This chapter presents the testing programme and main characteristics of the different test series, faying surfaces and measurements. A total of 19 specimens were tested. Plate thickness, material properties and bolts were identical whereas other parameters such as bolts' arrangement, holes' geometry and faying surfaces were varied to investigate their respective influences on the segment capacity and behaviour.

The clamping force was always provided by M30 TCBs of grade S10T (equivalent to grade 10.9 [11]) produced by TCB Limited in England [10] and all tested plates had a thickness of 25mm.

In most of the tests one plate had normal holes with a diameter of 33mm on the side of the bolt head while the other plate had one or two open slotted holes of the same dimension. Single cover plates were used in place of the usual washers under the nuts.

Table 1. Summary of the testing programme

	Resistance tests				
Reference	***WS-1x3***	***Z-1x3***	***Z-2x3***	***Z-1x6***	***Z-1x3n***
Nb. of Specimens	**5**	**5**	**3**	**3**	**3**
Bolt type	**TCB M30-110mm**				
Plate thickness	**25mm**				
Surface type*	**a**	**b**			
Nb. of rows	**1**		**2**	**1**	**1**
Bolts per row	**3**		**3**	**6**	**3**
Hole type	**Open slot, 33mm**				**hole, 33mm**
*** a: corroded weathering steel / b: ethyl silicate zinc rich paint**					

3.1 Test series

First two series of 5 tests (*WS-1x3* and *Z-1x3*) were performed to evaluate the two different faying surfaces. The geometry is shown below on Figure 3-1.

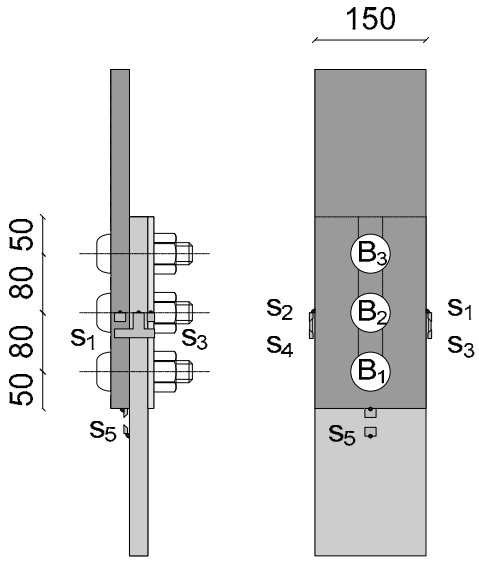

Figure 3-1. Specimens dimensions for series WS-1x3 and Z-1x3.

Then two new series (*Z-2x3* and *Z-1x6*) with the double amount of bolts were designed to study the group effect and influence of the bolt arrangement on the behaviour and resistance of the lap connection. Only the surface coated with ethyl silicate zinc rich paint was considered.
Series *Z-2x3* had two rows of three bolts. Three specimens were tested. The geometry is shown below on Figure 3-2.

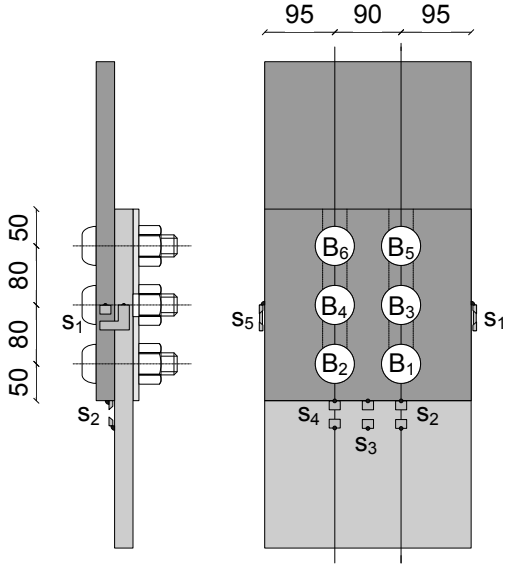

Figure 3-2. Specimens dimensions for series Z-2x3.

Series *Z-1x6* had one row of six bolts. Three specimens were tested. The geometry is shown below on Figure 3-3.

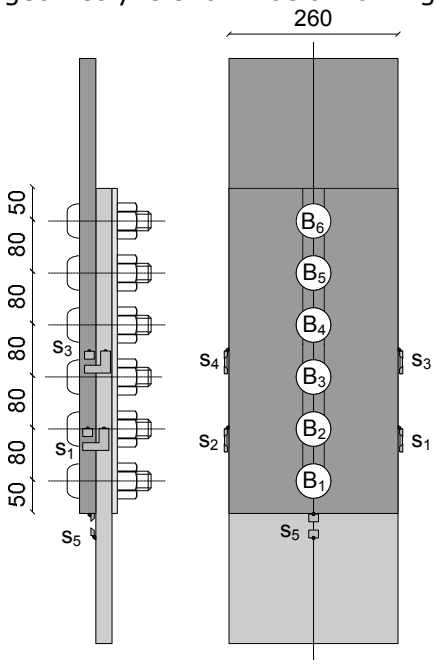

Figure 3-3. Specimens dimensions for series *Z-1x6*.

Finally a series (*Z-1x3n*) of three specimens with normal holes on both plates dealt as reference to estimate experimentally the effect of the slotted hole. Except for the holes, the geometry was identical to that of series *Z-1x3*. It is shown below on.

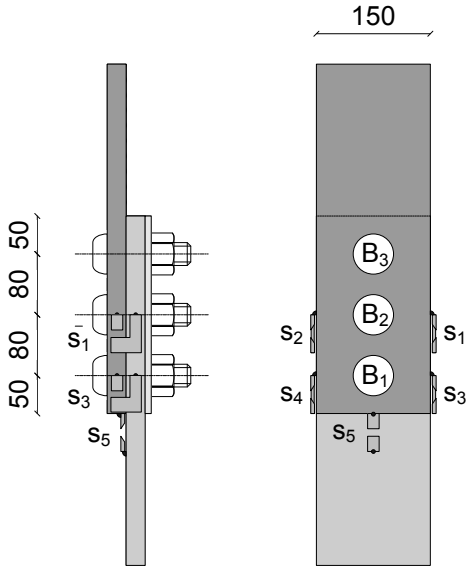

Figure 3-4. Specimen's dimensions for series *Z-1x3n*.

3.2 Faying surfaces

Two types of faying surfaces were considered: an ethyl silicate zinc rich paint that is already widely used as a primer for wind towers and weathering steel which provides a relatively high friction coefficient.

3.2.1 Ethyl silicate zinc rich paint

The plates were made of construction steel with grade S355 produced by *Ruukki*. They were first grit-blasted with steel grit of size G70 to a quality Sa2.5 according to ISO-8501-1[13] and then coated with the two component ethyl silicate zinc rich paint called *TEMASIL 90* produced by *Tikkurila Coatings*. According to the producer this coating has an excellent abrasion resistance and can be used as single coat or as primer. The zinc content is between 70 and 90%. A coat thickness of 50 to 80µm was requested.

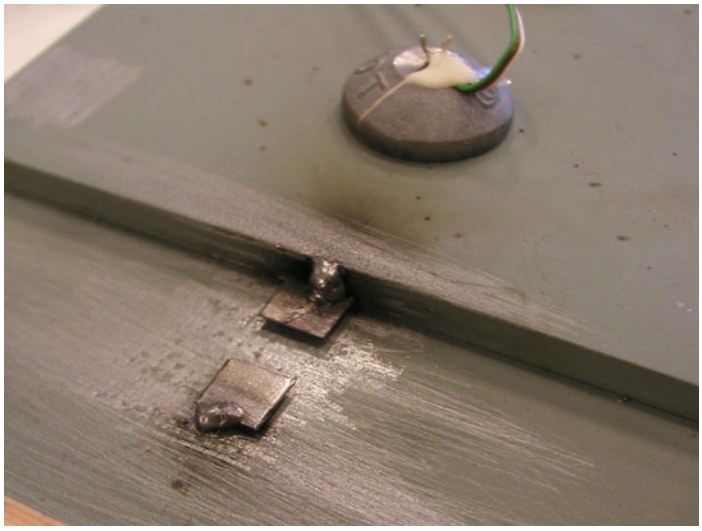

Figure 3-5. Ethyl silicate zinc coating appearance

3.2.2 Weathering steel

The selected material was COR-TEN B produced by *Ruukki* with material properties equivalent to a grade S355. The plates were first grit-blasted with steel grit of size G70 to a quality Sa2.5.

To obtain more uniform surfaces and repeatable conditions as well as to speed up the corrosion process, the plates were artificially corroded under controlled conditions. They were first sprayed with a mild solution of hydrochloric acid (HCl, about 2%) to initiate the corrosion process. Then they were sprayed twice a day with water for a period of 10 days. Enough time was provided between spraying for the surfaces to dry completely. The temperature was kept constant at about 10°C and the air humidity was very low. To facilitate runoff and avoid standing water the parts were kept somewhat upright. After artificial corroding the plates were stored indoors. It is therefore assumed that no further corrosion occurred.

3.3 Measurements

3.3.1 Applied load

The applied tensile load was accurately monitored by the testing machine load cell.

3.3.2 Bolt forces

The bolt forces were continuously measured during tightening and throughout testing in order to obtain information on the initial level of pretension, load relaxation, and variation and distribution of the clamping forces during loading of the specimens.

For this purpose strain gauges of type *BTM-6C* supplied by *TML* were installed in the bolts' shanks to monitor axial strains. They were then calibrated in tensile tests to obtain the relationship between measured axial strains and axial bolt forces.

3.3.3 Relative displacements

Relative displacements of points on different plates were measured to investigate the slip behaviour of the connection. This was recorded with Crack Opening Devices (CODs) measuring the relative displacements of knife-edges that were spot welded on the plates.

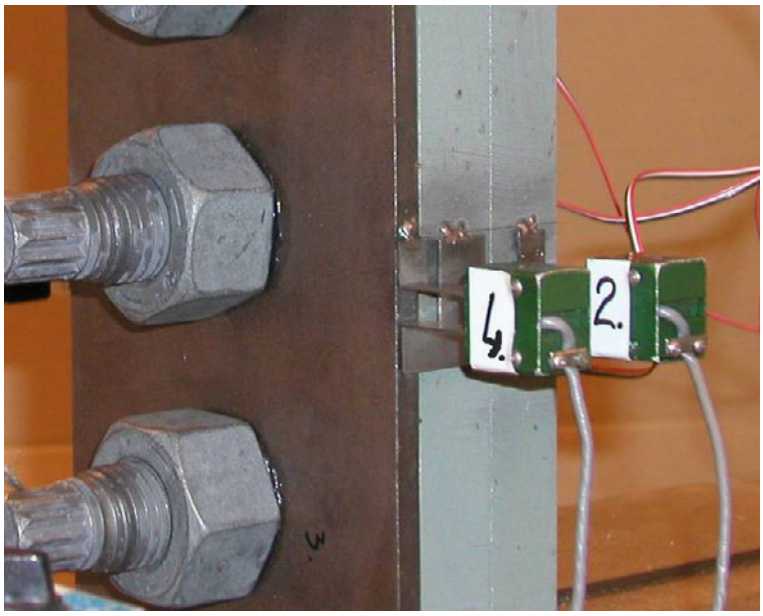

Figure 3-6. CODs measuring the relative slip of plates.

Measurements were always taken symmetrically on both sides of the specimens and an average slip was derived in order to account for possible in plane rotation of the plates.

3.4 Results

3.4.1 Behaviour of the lap joint in tension

Different geometries, bolts and faying surfaces lead to different responses of the specimens in terms of stiffness, resistance, etc. A qualitatively similar behaviour can be found for all. It is best described with an example.

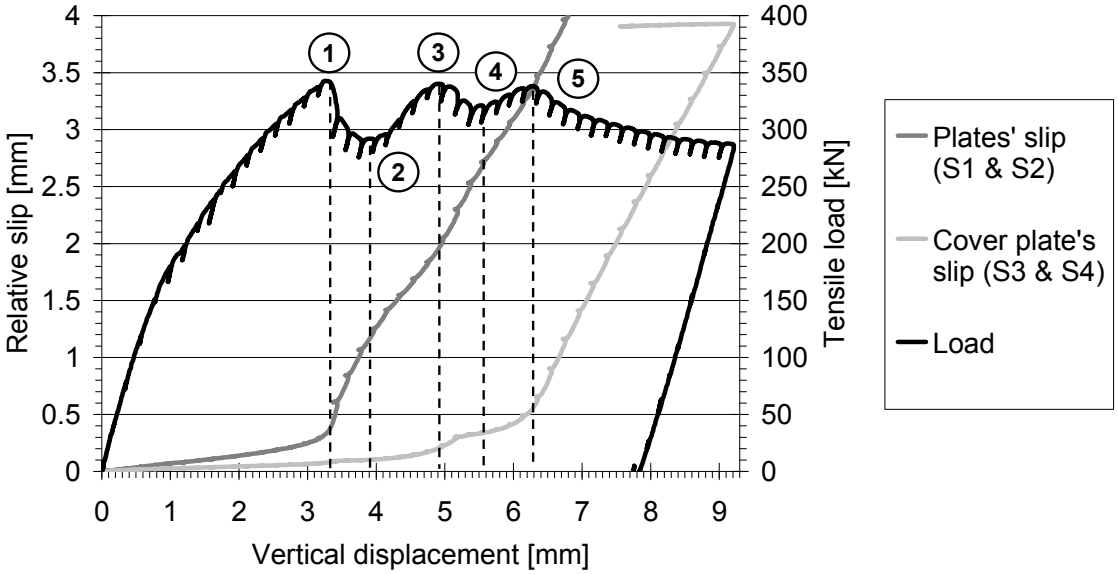

Figure 3-7. Load-displacement behaviour, example of specimen 2 from series *P-1x3*.

It appears that the behaviour is first linear but shows some nonlinearity at relatively low loads, already before the ultimate load (1) is reached. It should be noticed that the measurement of elongation is not accurate enough to derive the stiffness of the specimen and it should be regarded as indication only. It is unlikely that yielding of the plates occurs and if nonlinear deformations appear in the specimen they are certainly due to small relative slip (microslip) at locations away from the fasteners where the contact pressure is too low to transfer load by friction. At the ultimate load (1) friction is overcome over the whole contact area and the two plates slide relatively to each other (macroslip). At this point a sudden load drop is noticeable. It can be explained by a change from static to lower kinetic friction which may already be noticeable at low velocity [14].The post failure behaviour is then characterized by an increase of the transferred load after a certain amount of slip (2). At this point the cover plate still happens to "stick" to the underlying plate and the increase can be interpreted as the bolts bearing on the cover plate holes. As a result extra load can be transferred by friction between cover plate and underlying plate on one side, and between bolt heads and underlying plate on the other side. If the friction is lower below the bolt heads, which is the case here, the load can increase until a second drop (3) takes place as the heads start slipping. When they come in bearing (4) a last load increase can happen up to the point where the cover plates slips (5). If the friction below the cover plate is lower than between the heads only one

load increase may happen before the cover plate slips. The behaviour is schematized on Figure 3-8 below.

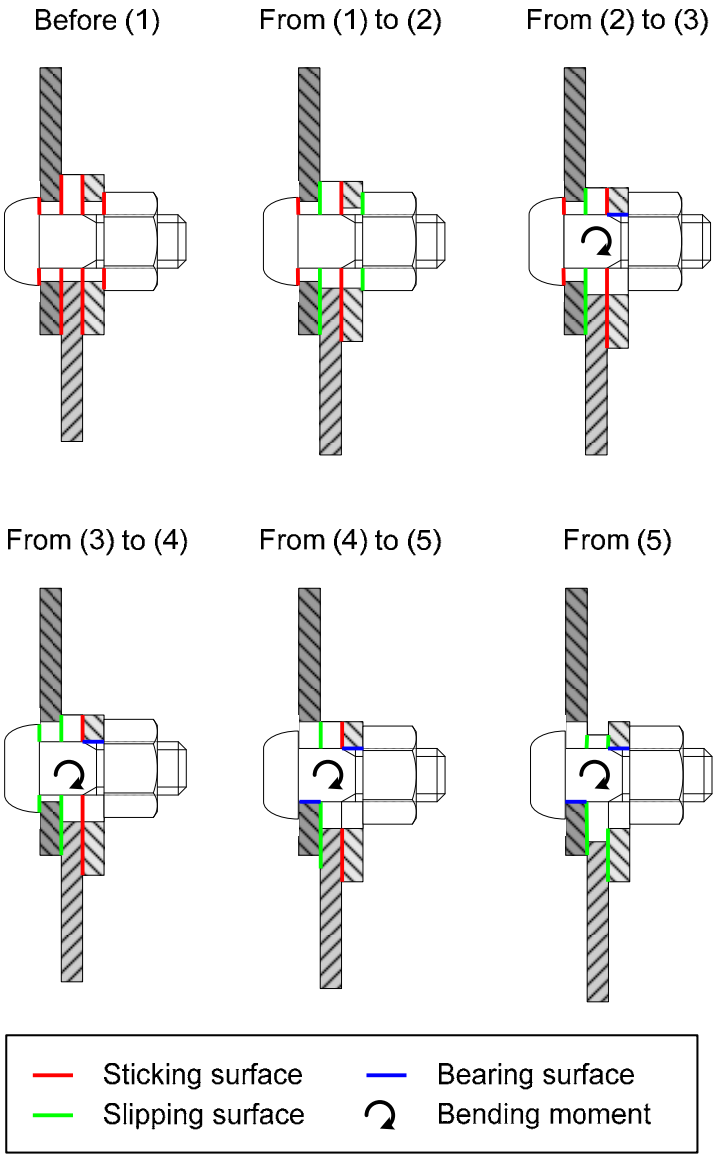

Figure 3-8. Schema of the post-slip behaviour. The bending moment due to non-symmetric connection exists from the beginning but it's influence is emphasized after a slip of approx. 1.5 mm.

3.4.2 Residual Bolts pretensions

The residual pretension is defined as the pretension remaining at test start. It is lower than the initial pretension defined as the bolt force present directly after tightening. Two effects contribute to the pretension losses:

Elastic interaction
The variations were negligible as the tightening was performed in two steps, from the stiffest location outwards.

Short term relaxation
The bolt forces presented a peak during tightening. Once the maximum was reached the forces decrease asymptotically. The magnitude of the pretension loss depends on the surface and plate thickness as well as on the geometry.

Series *Z-1x3* and *Z-1x3n* have identical surface properties, plate thickness and bolt size but the hole's geometry changes. From table 2 is clear that the influence of slotted holes on the average losses may be neglected.

Table 2. Evolution with time of the average loss of pretension of all bolts in % of the maximum.

Time after Max.	*Z-1x3*	*Z-1x3n*
10s	2.7	2.1
10min	5.7	5.0
12hrs	8.9	7.7

With a slotted hole, independently of the surface or specimen geometry the greatest losses are found at the central bolts (B2). This can however be reduced by tightening in two steps. The decreases are very similar for the leading bolts (B1 and B3) although there is a tendency for higher losses close to the slot opening (B3). With normal holes on both plates, the variations are very similar at all three locations.

3.4.3 Bolts forces variations in service

The bolts forces decreased when a tensile load was applied on the specimens. A correlation could be found between the variations of bolt force and the tensile load until major slip. At that point a sudden drop occurred. The losses were not recovered after unloading.

With the painted surfaces the achieved loads are relatively lower and the behaviour is quasi-linear. With corroded weathering steel nonlinearity develops at about half the specimen's resistance. It is more striking for the leading bolts.

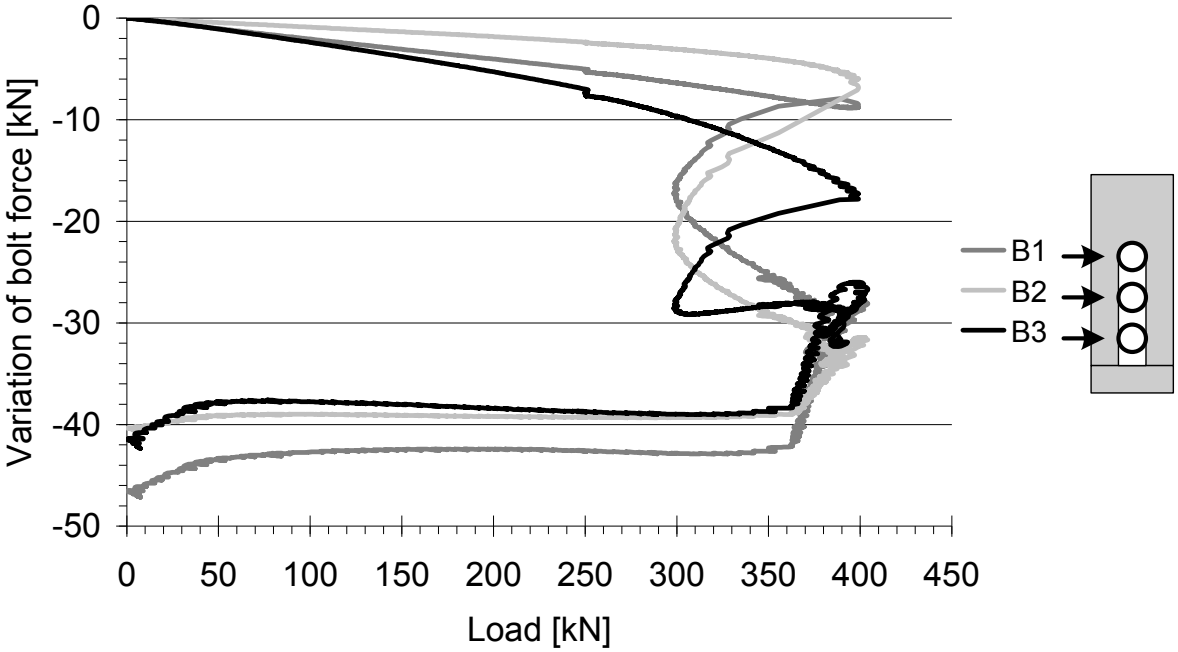

Figure 3-9. Bolts forces variations vs. applied load, example of specimen B from series *Z-1x3*.

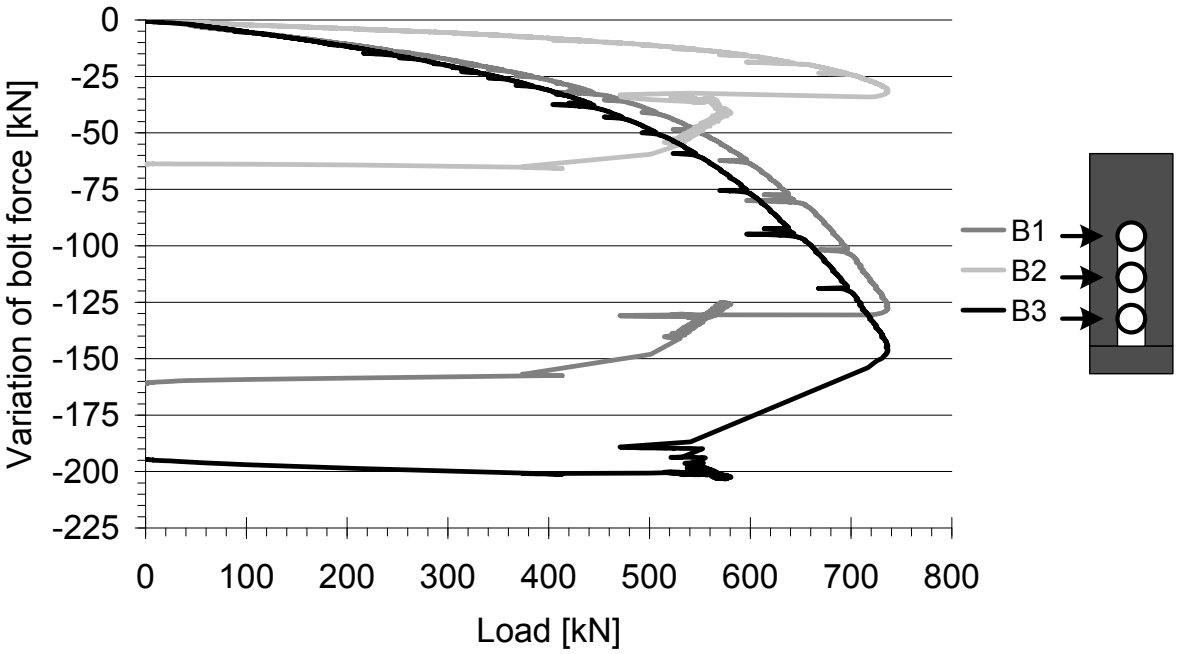

Figure 3-10. Bolts forces variations vs. applied load, example of specimen D from series *WS-1x3*.

The leading bolt at the close end of the long slotted hole (B1) behaves in a similar way as the equivalent bolt installed in a normal hole. The central bolts see the lower decreases of both series with roughly the same magnitude. Whereas the leading bolt at the open end of the slot (B3) looses the most force, the specimen with normal holes is symmetrical and both leading bolts have similar behaviours, i.e. the total decrease is slightly less important.

The variations of bolts forces of series *Z-1x3* and *Z-2x3* compare well. For series *Z-1x6*, the two leading bolts (B1 and B6) loose force quasi linearly as the load increases. Their loss rates are identical. They are higher than for specimens with three bolts only.

Qualitatively the leading bolts always loose more force than the central bolts. And the bolts closer to the slot's opening have higher losses than those close to the slot's closed end. In the long specimens (*Z-1x6*) the four central bolts loose the same amount of force. Some asymmetry is noticeable in the wide specimens (*Z-2x3*); higher losses are found in the row subject to additional tension from in plane rotation.

With comparable geometry and bolts the total clamping loss is more important for weathering steel specimens and the difference increases for thick plates with bigger bolts. The clamping loss is around 23% with corroded weathering steel, independently of the plate thickness and bolt diameter. For painted plates the loss was about 16% and 3 % for 8mm-thick plates with M20 bolts, and 25mm-thick plates with M30 bolts respectively.

The total loss of the wide specimens (*Z-2x3*) was very similar to that of the specimens with three bolts (*Z-1x3*). But the long specimens (*Z-1x6*) saw a decrease more than twice as high (about 8%).

The total losses are very similar between specimens with normal holes and slots. However the initial clamping forces and ultimate loads were higher with normal holes so that this configuration in fact leads to lower losses. The difference is noticeable at the slot end where higher losses were recorded.

3.4.4 Static resistance

The slip resistance of the connection was taken as the ultimate load, at occurrence of major slip.

The slip factor was defined as the ratio between slip resistance and initial clamping force. Note that the slip resistance has a different definition as given in EN1993-1-8 [15] and EN1090-2 [16]. Therefore the values given in the tables should not be compared directly to those available in the literature.

The apparent friction coefficient is defined as the ratio between the slip resistance and the sum of bolts forces at major slip. It allows a better comparison of the friction properties without accounting for the different variations of clamping forces.

Table 3 shows the average slip factors and apparent friction coefficients for all series.

Table 3. Slip factors and apparent friction coefficients.

Series	Z-1x3	WS-1x3	Z-2x3	Z-1x6	Z-1x3n
Slip factor	0.320	0.611	0.264	0.310	0.338
Apparent friction coefficient	0.356	0.795	0.288	0.337	0.370

Corroded weathering steel surfaces gave the best results. The slip factor was about two times higher than with ethyl silicate zinc rich paint. The variation is then about 1% compared to about 8% for the painted plates.

The slip factors from the specimens with a higher amount of bolts cannot be compared as the bolts did not have time to relax before test start. The apparent friction coefficients however show some differences. The specimens with one row of six bolts have an apparent friction coefficient lower by only 5%. The loss is much more important, about 20%, with two rows of three bolts.

These results may be attributed for one point to the small amount of specimens. Other reasons may be related to testing conditions. Indeed it could be noticed that in plane rotation occurred. The direction of rotation was identical for all specimens tested in each load frame. It is thus reasonably assumed that it was introduced by misalignments in the tensile machines. It was greater for the WOLPERT load frame used for series *WS-1x3*, *Z-2x3* and *Z-1x6*. And while the influence can be neglected for narrow specimens, the associated strains grow with the specimen width and may have an influence on the behaviour of the wider specimens of series *Z-2x3*. At major slip the average in plane rotation was about $1.6.10^{-3}$ radians. For the smaller specimens that were tested in the other load frame the average rotation was about half as high.

The resistance of specimens with normal holes was relatively about 4% higher than that of equivalent specimens with long slotted holes. The results variation also was lower. Due to the small amount of specimens the confidence interval is however small. More tests would be required to obtain statistically relevant results.

3.4.5 Effects of eccentricity

All tests were performed on single lap joints and the load was thus introduced eccentrically creating some out of plane bending. In a wind tower application the plate curvature would create some three dimensional restraint and the behaviour may thus be different from that of the unrestrained segment joint [9].

It was not possible within this framework to investigate these effects experimentally.

4 Numerical analysis

Important test parameters such as the contact pressure or the stresses in the plates are inconvenient or impossible to obtain experimentally. Advanced numerical models were thus used to estimate these quantities and allow a more thorough analysis.

Three dimensional finite element models of the test specimens were created using the commercial software *Abaqus 6.7.1*. They were calibrated with experimental results.

4.1 Contact pressure distribution

The contact pressure distributions with slotted and normal holes are shown on Figure 4-1 and Figure 4-2 respectively. The contact zones and wear patterns are in good agreement. The spread of the contact zone is very similar, independently of the hole's type.

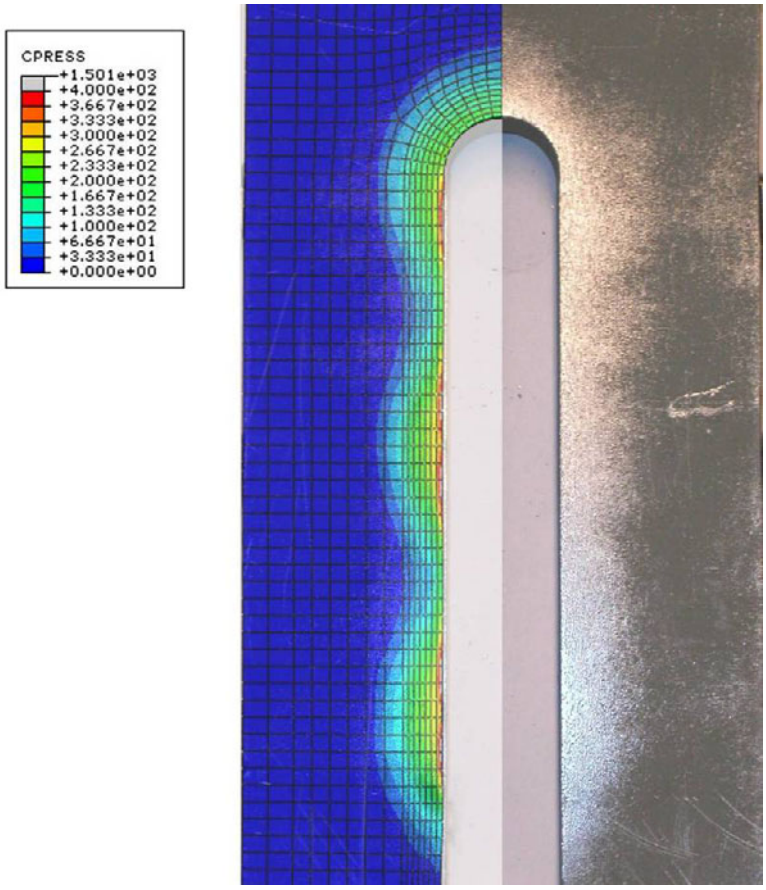

Figure 4-1. Comparison of contact pressure distribution and wear pattern of the plate with slotted hole (*Z-1x3*).

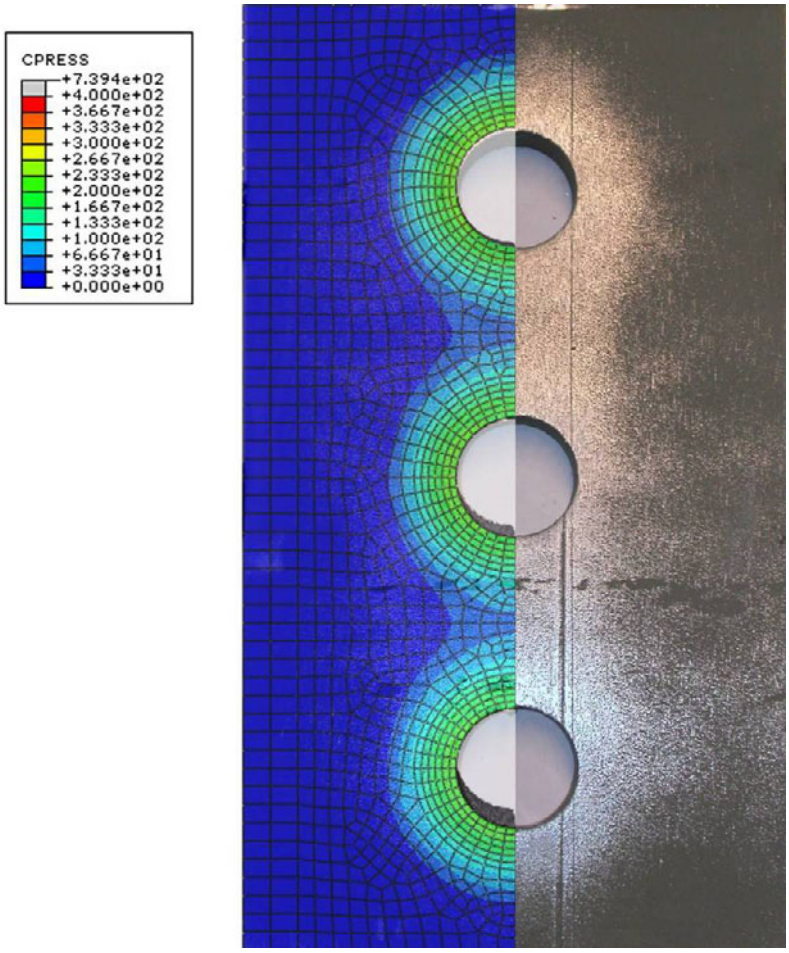

Figure 4-2. Comparison of contact pressure distribution and wear pattern of the plate with normal holes (*Z-1x3n*).

The pressure decreases from a maximum at the hole's edge to about zero at the edge of the contact area.
With normal holes there is no difference between the pressure distributions under the different bolts. The maximum pressure is about 220MPa, i.e. about 72% of a uniform pressure under the bolt head. It decreases first slowly and then more rapidly and linearly. These results compare well with experimental results found in the literature [17].
With a slotted hole, as the lateral contact spread is identical, the contact area necessarily is smaller and the pressure is then higher to resist the same clamping force. It is lower for the bolt at the closed end (B1) for which the contact area is closer to that with normal holes. The pressure distribution is very similar under the two other bolts. The maximum are about 260MPa and 360Mpa, i.e. about 95% and more than 120% of a uniform pressure under the bolt head, for B1 and, B2 and B3, respectively. The decrease appears more linear.

4.2 Mechanism of load transfer

Figure 4-3 shows the evolution of the contact shear stress distribution with the transferred load at the three bolt elevations for series *Z-1x3*. For loads well below the static resistance of the connection two zones are observed which correspond to slipping and sticking conditions. In the first the shear stress is equal to the product of the contact pressure and the friction coefficient. Its magnitude increases linearly and reaches a maximum at the boundary between slipping and sticking regions. In the sticking area the contact shear stresses decrease towards the hole edge where constraints are maximal.

Before the static resistance is reached the behaviour is similar at both leading bolts. The force transfer proceeds from the joint edge towards the centre.

First the shear stresses increase at the leading bolts while they remain lower and quasi constant at the central bolt. Once the whole contact area under the leading bolts is slipping, deformations of the plates lead to an increase of the shear stresses transferred under the central bolt until major slip of the connection.

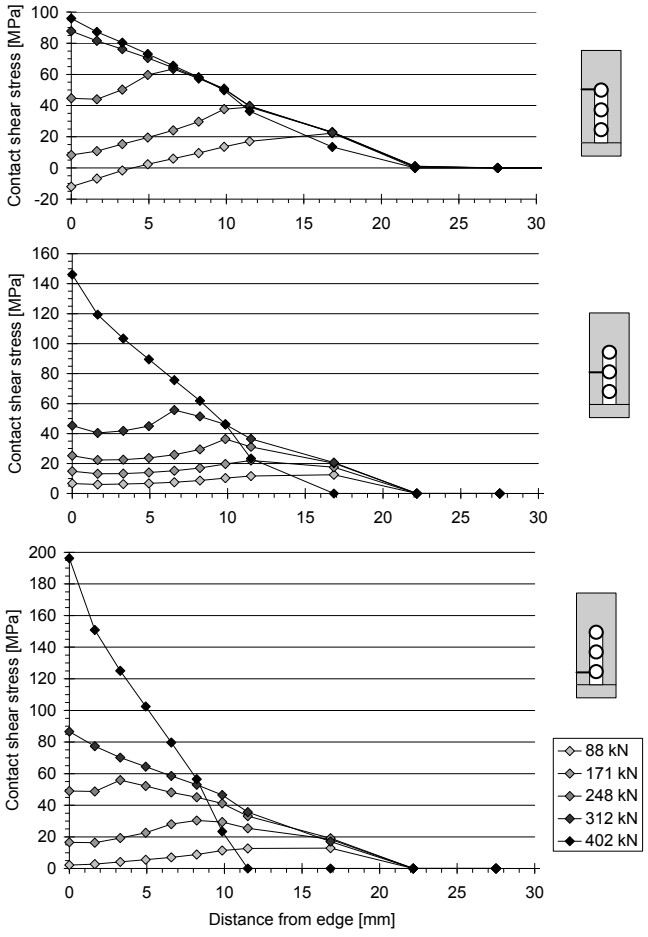

Figure 4-3. Evolution of contact shear stress distribution with transferred load at the three bolt elevations: a) B1; b) B2; c)B3.

With increasing loads the bending moment induced by the joint eccentricity introduces out-of-plane deformations (See Figure 4-4). This three dimensional bending of the plates slightly modifies the contact pressure distribution: the contact area decreases and the maximum pressure increases. The phenomenon is more noticeable towards the slot opening. It explains the increased shear stresses at the highest load under bolts B2 and B3.

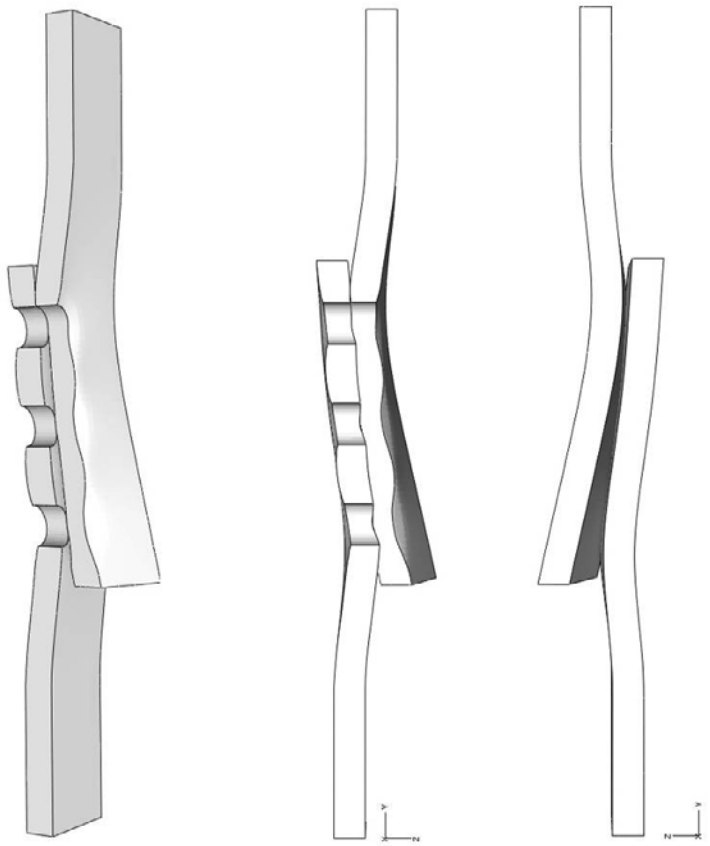

Figure 4-4. Plates deformations at the ultimate load of 402kN (magnification factor across the plate thickness: 100).

4.3 Evaluation of the plate stress distribution

The stresses in the plates are not uniform. Due to eccentricity bending stresses are observed.

On Figure 4-5 the tensile stress component (about the y-axis) for different transferred loads is plotted at different elevations across the contact face of series *Z-1x3*. For loads well below the slip load the stresses are higher at the edge of the sticking zone and decrease towards the hole's edge.

In general they increase from the third to the first bolt as more shear force is introduced under the consecutive fasteners. A zone of higher magnitude is

found around the closed end of the slot (See also Figure 4-6). After that the stresses are more evenly distributed and as the net cross-section increases the magnitude decreases.

The tensile stress concentration around the leading bolt is consequent with fatigue failure modes reported in the literature [18] where fatigue cracks originated from a zone in front of the leading hole.

The normal surface stresses at the connection's edge are slightly concentrated around the slot's axis. The maximum ratio between average and maximum stress is about 1.17.

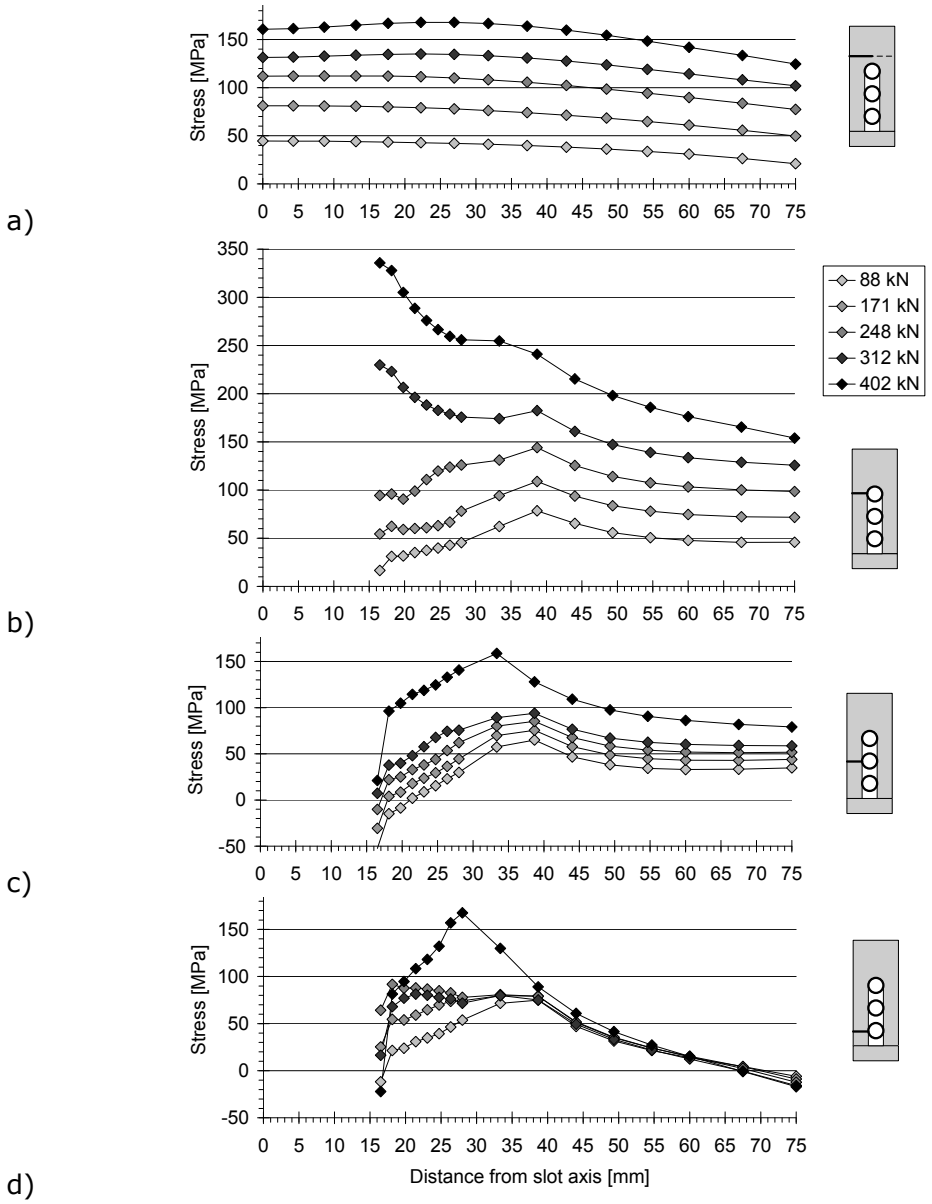

Figure 4-5. Evolution of tensile stress component distribution with transferred load at four elevations for series *Z-1x3*: a) joint edge; b) B1; c) B2; d)B3.

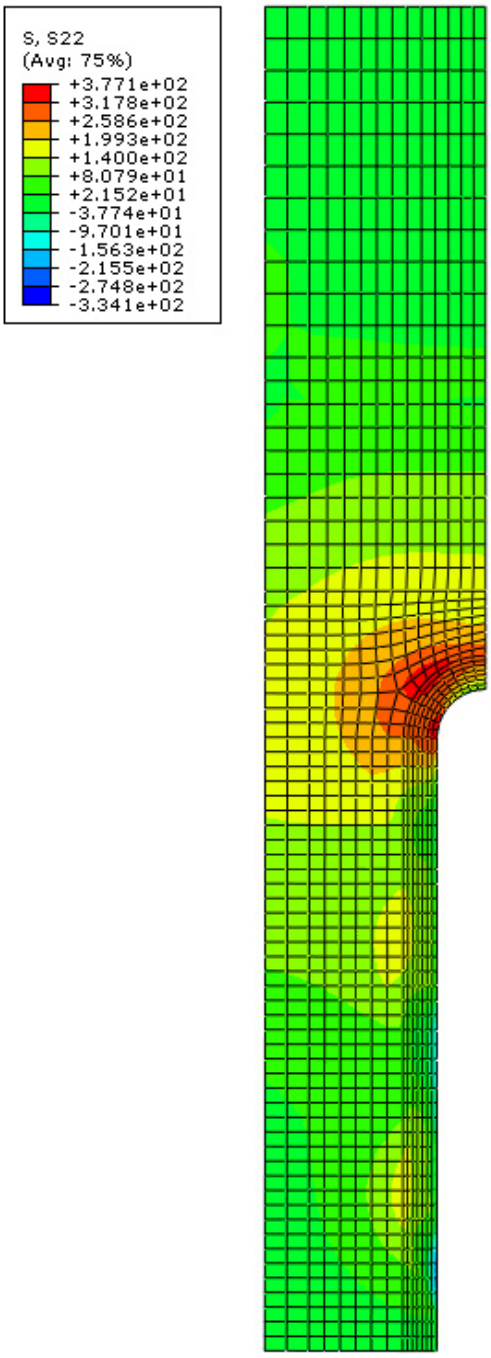

Figure 4-6. Tensile stress component distribution at the ultimate load for series *Z-1x3* (*test-25mm-slot-11*).

5 Long term tests

The long term behaviour of the specimens was investigated in a series of tests to determine the variations of bolt forces and creep of the plates with time.

Six specimens were loaded for a period of four months, three at 80% and three at 60% of the expected static resistance. The tests were divided in four steps: loading, creep, unloading and resistance

5.1 Measurements

5.1.1 Bolt forces

The bolt forces were constantly recorded with help of strain gauges inserted in the shank as for other test series.

5.1.2 Relative displacements

The relative displacements were measured with help of Crack Opening Devices during loading, unloading and final testing. During long term testing the displacements were measured with a *Staeger* device.

The displacement measurements are relative variations between knife-edges or steel balls for each test step. Absolute values were defined setting the initial distance at the beginning of the loading step as zero. The different steps were then combined by interpolation.

5.2 Test setup

Special rigs were designed for the long term tests. The load could be applied on each specimen independently. To avoid introducing torsion the load was applied by pulling the upper threaded bars with a hydraulic jack. The nut was then snug tightened by hand and retained the load when the pressure in the jack was released.

To reduce the stiffness of the assembly and thus ensure a relatively constant load three spring washers were used. For a relative slip or settlement of 1mm the load would decrease by 30kN only.

Figure 5-1 shows two test rigs and the loading setup with the hydraulic jack and controlling load cell installed.

Figure 5-1. Loading setup.

Elongations due to settlements and creep induced only small load changes with an average variation of 1.2% and a maximum of 2% after four months. The applied load could thus reasonably be considered as constant.

5.3 Results

5.3.1 Bolt forces

After the specimens were loaded the bolt forces kept decreasing. No significant difference was observed between the specimens with different loads. The losses appeared asymptotical and reached about 4% after 15 weeks. Assuming an average logarithmic decrease rate of about 15kN.log(s)$^{-1}$ the additional clamping loss over a 20 years period was extrapolated to about 30kN, i.e. about 3% of the initial preload.

5.3.2 Plate creep

Under constant loading the plates underwent relative slip with time. Its magnitude was higher closer to the joint ends, i.e. at the leading bolts elevations. Creep was more important for the higher load.

Most creep happens during the first hours and seems to stop after one to two weeks. Delayed slip after three hours exceeded the value of 2µm and extended creep tests should be performed according to EN1090-2.

"Displacement – log time" curves were derived and the delayed slip for a lifetime of 30 years was extrapolated. None of the delayed slip exceeded 100µm which is well below the accepted limit of 300µm.

Although the service load was 80% and not 90% of the expected resistance the delayed slip is so small that it is not likely to be design driving and a reduction of the slip factor is not necessary

5.3.3 Remaining static resistance

The remaining resistance of the specimens subject to long term loading was lower than that of equivalent new specimens by about 10% in average. Part of the loss can be related to long term relaxation of the bolts. But this accounts only for about 4%. The rest is thus related to the faying surfaces which is also recognizable by the lower apparent friction coefficient.

The specimens subject to the lowest loads contradictorily showed the highest difference. The statistical relevance of the results is thus questioned. More tests would be required to confirm the above mentioned hypothesis.

5.3.4 Concluding remarks for the friction connection design

Based on testing program on connections that consisted of:

- 9 preliminary tests,
- 19 main tests,
- 12 long-term tests,
- 10 standard friction tests,
- 50 pre-tension test,

following conclusions are made for reduction of pre-tension force in the TCB bolts in open slotted hole with the cover plate (having the same material properties as the washer):

- elastic interaction, may be neglected;
- the biggest short term relaxation is with the zinc paint, -9%,
- long term relaxation over the life time (20 years) -7 %,
- relaxation in service because of the plastic deformation of asperities -3 %.

Further conclusions are:

- The total loss of the pre-tension force in the bolts approximated as 20 % in the considered connection.
- The slip factor for the corroded weathering steel is 0.6 and 0.3 for ethyl silicate zinc rich paint.
- Design resistance values based on testing are increased for 14 % compared to the nominal values according the Eurocode, EN-1993-1-8.

6 Cyclic temperature

The influence of temperature cycles on the pretension force of the bolts in the connection was investigated in total four specimens, three of them loaded in tension and one of them as unloaded reference. A temperature range from room temperature, around 18 °C, to -22 °C. The cooling was performed in a climate chamber and the warming in the room in front of it. The warming was speed-up by a fan which produced continues air stream.

The loaded specimens have the index G, H, I and the unloaded index J. The bolts have a clamping length of 58 mm. This value was used to calculate the strain in the temperature range.

The strain was measured with strain gauges of the type BTM-6C. This strain-gauge is special designed for strain measurements in bolts. The strain-gauge has an operational temperature range from -10°C till +80°C. The lower boundary is a bit out of the temperature range. The adhesive used to glue the strain-gauge has a temperature range from -30°C till +100°C.

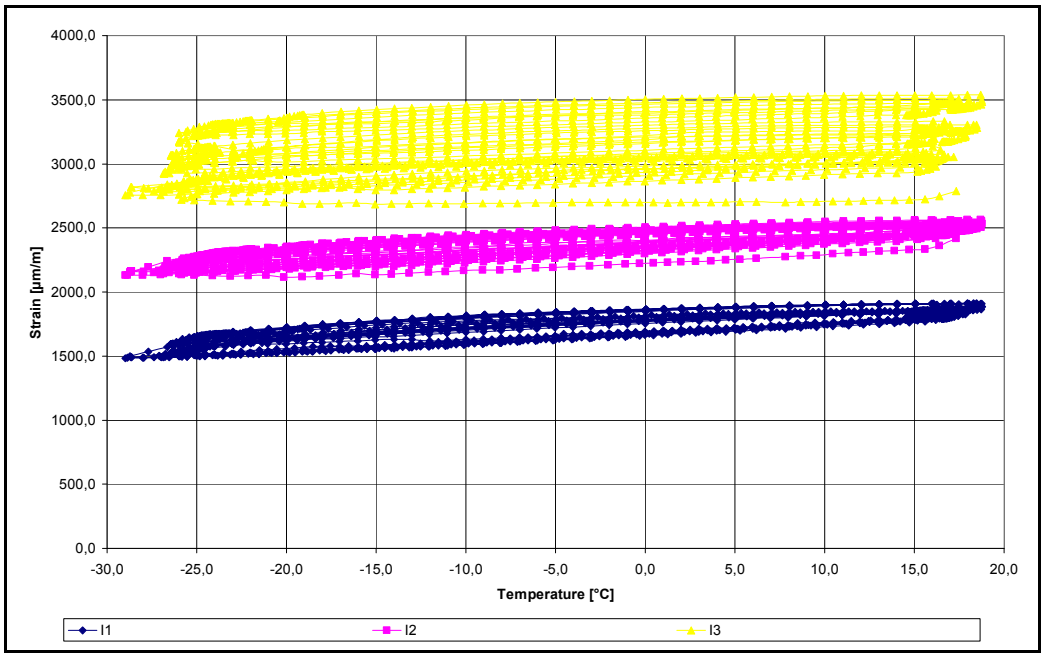

Figure 6-1 Results of temperature variation in the specimen I

Table 4. Overview of the experimental results

	Temperature difference [°C]	Specimen G3 [µm]	Specimen GL [µm]	Specimen H1 [µm]	Specimen HL [µm]	Specimen I1 [µm]
Average	39,9	18,8	20,1	22,9	19,0	18,5
Standard deviation	0,4	0,8	0,6	0,7	0,6	1,5
	Temperature difference [°C]	Specimen I2 [µm]	Specimen IL [µm]	Specimen J1 [µm]	Specimen J2 [µm]	Specimen J3 [µm]
Average	39,9	19,1	19,2	20,3	20,8	18,8
Standard deviation	0,4	0,8	0,5	0,5	0,5	0,4

Based on the results shown in Table 4 which shows that the stress level difference generated in cyclic temperature is about 1% of the yield strength, influence of the temperature variation may be neglected in the "HSIWTIN" friction connection.

7 Design recommendations

7.1 Introduction

The design resistance of EN1993-1-8 [15] for High Strength Friction Grip connections with a single friction surface is given by:

$$F_{S,Rd} = \frac{k_S}{\gamma_{M3}} \mu \sum_{bolts} F_{p,C} \qquad \textit{(7.1)}$$

Where, k_S is a correction factor,

γ_{M3} is a partial factor taken as 1.25 ,

μ is the slip factor obtained from predefined categories or from standardized tests according to EN1090-2, and,

$F_{p,C}$ is the bolt characteristic pretension.

The value of the correction factor varies with the hole's geometry. For long slotted holes with their axis parallel to the direction of load transfer k_S=0.63.

The correction factors are empirical and have their roots in investigations led in the late '60s by Allan and Fisher [8], and, Shoukry and Haisch [7]. It should be noticed that the specified initial pretension is used in the resistance formulae. The correction factors therefore account for different residual pretensions, bolt forces behaviours and apparent friction coefficients. All of these are influenced by numerous parameters and it appears hardly possible to provide a general set of correction factors that will give efficient design for all configurations. More advantageous correction may thus be derived for specific applications.

7.2 Determination of the correction factors

The standard procedure for statistical determination of resistance models described in Annex D of EN1990 [19] was used to derive specific reduction factors from the experimental results.

The specimens which were previously loaded for a period of 15 weeks showed lower remaining resistances and were thus conservatively considered in the calculation.

The coefficient of variation of the friction coefficient was estimated from the friction tests and taken as 12%.

The coefficient of variation of the initial pretension of a single bolt is taken as 7%, based on the worst case from the test requirements for TCBs. Thus the variation of total initial pretension was taken as 4%.

From friction tests, the experimental slip factor was found to be μ=0.45 and the correction factor was derived as k_S=0.64. The slip resistance achieved for a pretension of 1kN is thus:

$$\mu.k_S = 0.45 \times 0.64 = 0.288\ kN$$

According to EN1090-2, components coated with zinc rich paint have surfaces of category B, i.e. μ=0.4. For long slotted holes with their axis parallel to load transfer k_S=0.63. According to EN1993-1-8 the slip resistance achieved for a pretension of 1kN is thus:

$$\mu.k_S = 0.4 \times 0.63 = 0.252\ kN$$

The design slip resistance could be improved by about 14%.

For the specimens with normal holes the experimental design resistance is 17% lower than the design resistance according to EN1993-1-8. It appears that the slip factor given in EN1090-2 for zinc rich paint is too high when bolts with large diameters are used

7.3 Recommendations

7.3.1 General

The correction factors account for the influence of parameters which vary between the specimens used to determine the slip factor and the designed application. To ensure safe and easy design the standard values are necessarily too conservative in most cases and design by testing is thus beneficial.

The slip factor should be determined experimentally under conditions close to the final solution. Clamping force and plate thickness are parameters of primary importance. They should be identical to those of the considered application.

More appropriate correction factors can then be derived and associated to the specific test conditions.

7.3.2 Specific case

For the specific application considered here it is recommended to use a correction factor of k_S=0.64 together with a slip factor μ=0.45 for ethyl silicate zinc rich paint.

In absence of long term tests it can be assumed that the clamping force will decrease by about 15% over a period of 20 years. The correction factor obtained from static tests should be adapted accordingly.

8 Design example and cost analysis

The implementation of friction connections in wind towers is considered in this chapter. The design of wind towers is presented with focus on the connections. The design of L-flange connections is reviewed and a method is given to dimension friction connections and determine their resistance to static and fatigue loads.
The design methods are illustrated in an example of a real wind tower, see Figure 8-1, which is also used as basis for a cost analysis of both solutions.

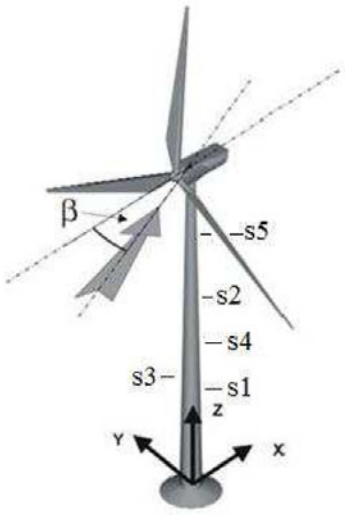

Figure 8-1. MM92 Tower produced by REpower, Portugal, consist of three parts and two flange connections, position S1 and S2

8.1 Wind tower design

8.1.1 Design loads

The static design loads usually are derived from information on the wind speed and direction with help of simplified models including the geometrical properties of the tower. Many Design Load Cases (DLC) are simulated which include the relevant combinations of turbine configuration and wind.

The fatigue loads are derived in the time domain by a simulation programme. The results are time series for different load cases and for all load components. To simplify the fatigue design a rainflow count is performed. The result is a rainflow matrix. For linear systems only the load range is required and the matrices can be simplified into load spectra by removing the information on the mean. A final simplification is then the derivation of a Damage Equivalent Load (DEL) that can be used as a static load.

8.1.2 Design of bolted ring flange connections

For design purpose it is assumed that the resistance of the three dimensional bolted ring flange connection can be described by the resistance of a segment with a single bolt which is loaded in tension.

The resistance at the Ultimate Limit State (ULS) is governed by yielding of the bolts or development of plastic hinges in the shell or flanges. Engineering models have been developed to estimate the resistance to the different failure modes.

The fatigue resistance is governed by the failure of the bolts. The applied loads are dependent on the geometry and their estimation is complex due to the nonlinearity of the phenomena.

A more thorough description of the design methods can be found in [20].

8.1.3 Design of friction connections

To design a friction connection the same approach can be used as for the design of flange connections, i.e. a segment with a single row of bolts is considered.

The static resistance at the Ultimate Limit State can be defined as the slip resistance.

It can be shown that with the assumption of a uniform stress distribution in the connection segments, the minimum number of bolts required in the connection is given as:

$$n_{Bolts} \geq \frac{\sigma_{N,Ud} \cdot \pi \cdot d_a \cdot s}{F_{S,Rd}} \qquad \textbf{(8.1)}$$

So it becomes evident that the considered case is that of pure compression giving an equivalent maximum stress. In reality the connection is loaded mainly in bending and the segments closer to the neutral axis will support much lower stresses unless the plastic resistance of the sections can be developed. Redistribution of the loads will thus certainly lead to higher resistances and this assumption can be considered as safe.

The maximum number of bolts rows is determined alternatively by the spacing defined in EN1993-1-8 or by the clearance necessary for the tightening tools. The electrical wrenches used to tighten Tension Control Bolts are relatively compact and with this type of fastener the spacing limits will be set by EN1993-1-8. The minimum distance between bolts rows is thus:

$$p_2 = 2.4 \cdot d_H \qquad \textbf{(8.2)}$$

The maximum number of bolts rows becomes:

$$n_{rows} \leq \frac{\pi \cdot d_a}{2.4 \cdot d_H} \qquad \textbf{(8.3)}$$

The minimum amount of bolts per segment is easily obtained. It should then be rounded to the next integer and with this number a new amount of rows can be calculated. It should satisfy (7.15).

Although a segment of the friction connection looks like a lap connection, it actually has three dimensional constraints from the shell curvature that will prevent out-of-plane bending. For fatigue calculation it can thus be regarded as a "one sided connection with pretensioned high strength bolts". For this type of detail the category 90 is used according to EN1993-1-9 [4]. Following the recommendations of Germanischer Lloyd Guideline [2], the endurance limit at 10^8 cycles should be disregarded.

Table 5. Properties of the Wöhler curve considered for the friction connection.

$\Delta\sigma_C$ (N=2.10^6)	$\Delta\sigma_D$ (N=5.10^6)
90.0	66.3

The damages can be derived with:

$$N_i = \begin{cases} N_C \cdot \left(\dfrac{\Delta\sigma_C}{\Delta\sigma_i} \right)^3 & if \quad \Delta\sigma_i \geq \Delta\sigma_C \\ N_D \cdot \left(\dfrac{\Delta\sigma_D}{\Delta\sigma_i} \right)^5 & if \quad \Delta\sigma_i < \Delta\sigma_D \end{cases} \qquad \textbf{(8.4)}$$

The considered area for the derivation of the stresses is the gross area. A single Wöhler slope with m=4 may be used as it is current practice for wind towers. This significantly simplifies the fatigue calculations as DEL can be used. A partial safety factor, γ_M , must be applied to the calculated stress range. It was taken as $\gamma_M = 1.25$

8.2 Design example

The tower considered in this example is of the type *MM92* produced by *REpower*. Its hub height is 80m and it supports a three blade turbine with a diameter of 92.5m and a nominal output of 2MW. It was built in Marvila, Portugal and is designed for wind class II_A according to the international standard IEC 61400-1, second edition 1999-02, and the German DIBt guideline, edition 2004.

The tower is made of three sections assembled with two intermediate L-flange connections. The actual solution is presented and alternative friction connections are designed based on the design loads provided by REpower.

Only longitudinal stresses were considered in the design and the static loads applying on the two connections can be simplified as in Table . The values include a safety factor taken as 1.35.

Table 6. Extreme design loads at the flange sections.

	Fz	Mr
	kN	kN.m
Flange2	-1846	25221
Flange1	-2443	48631

The fatigue loads were provided by REpower as Damage Equivalent Loads (DEL) for each load component for different Wöhler slopes. For tubular wind towers made of steel it is current practice to use m=4. Only damages from tensile stresses were considered and the damage loads were simplified as in Table 7.

Table 7. Damage Equivalent Loads at the flange sections (m=4 and $N_{ref}=2.10^8$).

	Fx	My
	kN	kN.m
Flange1	96	4243
Flange2	81	2359

8.2.1 Flange connections

The properties of the current flange connections are shown on Figure 8-2and Figure 8-3.

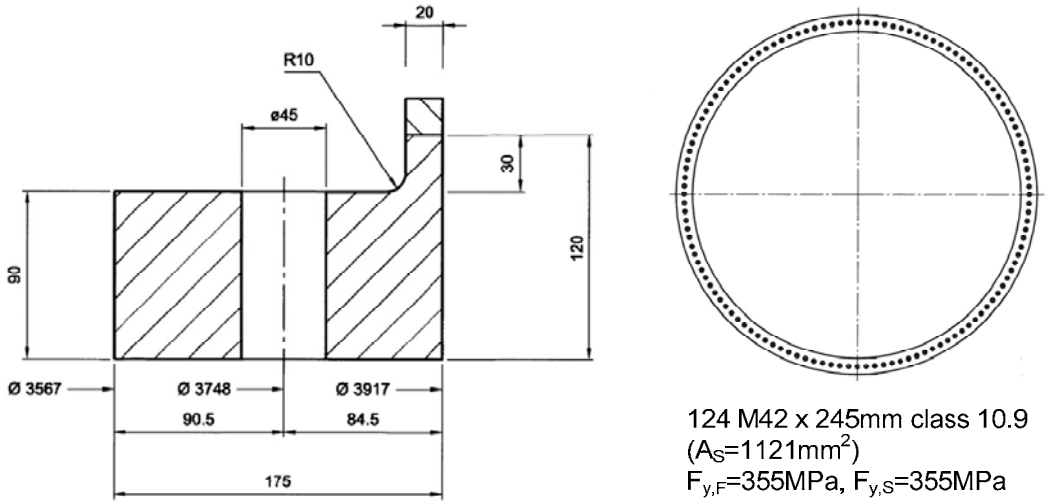

Figure 8-2. Flange 1.

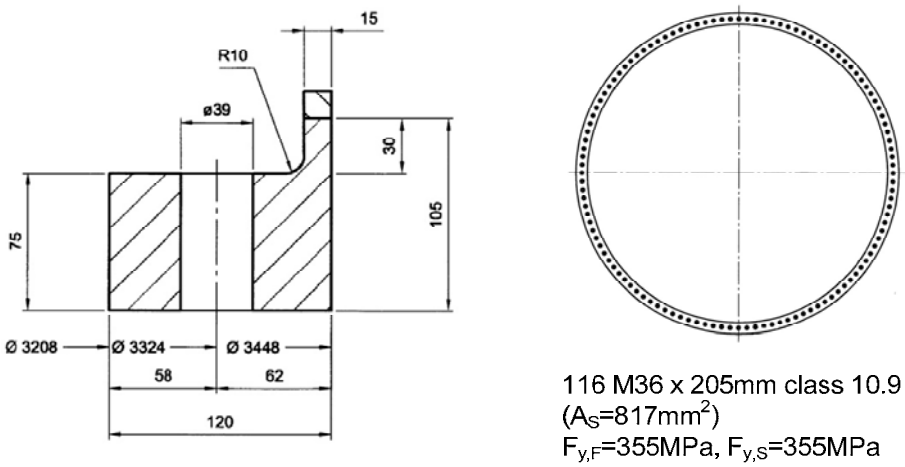

Figure 8-3. Flange 2

The design method presented by Seidel in [1] was used to assess the static resistance of the flange connections. The results are shown in Table 8.

Table 8. Design resistances of the flanges.

	Failure mode	Ultimate resistance [kN]	Design action [MPa]	Design action/Design resistance
Flange 1	Plastic hinge in the shell	552	290	0.67
Flange 2	Full plastification of the shell	436	322	0.53

Unfortunately the rainflow matrix of the fatigue loads for the tower was not available. Thus it was not possible to perform a fatigue check of the flange connections.

8.2.2 Friction connections

The friction connections are dimensioned to resist the tensile stresses induced by the design loads. The results are presented in Table 9.

Table 9. Optimum dimensions and static resistances.

	Flange 1	Flange 2
No. of bolts	**588**	**351**
Bolts per row	4	3
No. of rows	147	117
Spacing [mm]	84	93
Design action [MPa]	216	196
Design action/Design resistance	0.99	0.99

In the considered configuration the friction connections have a sufficient strength to resist the ultimate design loads. If needed it would be possible to increase the number of bolts to obtain a resistance equivalent to the yield strength of the cross section.

The fatigue strength is verified with help of the Damage Equivalent Loads provided for the considered tower. First the fatigue stress at 2.10^8 cycles is calculated from the Wöhler curve with a slope m=4:

$$\Delta\sigma_N = 90 \cdot \left(\frac{2.10^6}{2.10^8} \right)^{1/4} \approx 28.5\ MPa$$

The damage equivalent tensile stresses in the gross cross-section are then derived considering only the tilting moment My. The results are shown in Table 10. The damage equivalent stresses are compared to the fatigue strength. Both connections have sufficient strength and margin of more than 20%.

Table 10. Fatigue strength.

	Connection 1	Connection 2
$\Delta\sigma_{N,DEL}$ [MPa]	22.4	21.4
$\Delta\sigma_{N,DEL} / \Delta\sigma_N$	0.79	0.75

8.2.3 Comparison

For a given surface the static resistance of the friction connection is determined by the total amount of bolts. Whereas the number of bolt rows is limited by a minimum spacing, it is possible to increase the number of bolts per row in order to achieve the required resistance. The example showed that, with a realistic amount of relatively small bolts, connections could be designed with a resistance exceeding the yield strength of the base material.

The flange connections actually used have sufficient resistances but the margin for improvement is more limited as even bigger bolts and thicker flanges would be necessary.

Using friction connections, the tower resistance to static loading can thus be shifted to material strength or stability, both of which may be improved by using higher steel grades and carefully designed cross-sections.

The friction connections designed in the example had, according to EN1993-1-9, sufficient fatigue strength. Unfortunately the rainflow matrices were unknown and it was not possible to directly compare the total damages for both alternatives.

The single damages on friction connections are independent of the average stress. The influence of stress ranges with low average is thus higher and vice versa.

The fatigue strength of the friction connection should be investigated experimentally to determine the detail category. Benefits may be gained over the current recommendations from EN1993-1-9. In any case the fatigue strength of friction connections can be improved by increasing the shell thickness while the fatigue strength of the flange connection is limited by bolt and flange size limits.

8.2.4 Cost analysis

The material costs for both solutions can be compared and other construction aspects are discussed qualitatively.

Table 11 and

Table 12 show the material costs for both flange connections. The price information was provided by *REpower* in December 2007.

Table 11. Material costs of flange connection 1.

Component	Unit price [€]	Amount	Total Price [€]
Flange (d_a=3917mm)	6762.00	2	13524
Bolt (M42x245 10.9)	20.32	124	2520
		Total:	**16044**

Table 12. Material costs of flange connection 2.

Component	Unit price [€]	Amount	Total Price [€]
Flange (d_a=3448mm)	4395.00	2	8790
Bolt (M36x205 10.9)	11.40	116	1322
		Total:	**10112**

Table 13 and

Table 14 show the material costs for both friction connections with ethyl silicate zinc rich paint. The prices of Tension Control Bolts were based on a quote from *TCB Ltd* for 1000 pieces dated from August 2007.

Table 13. Material costs for friction connection 1 with ethyl silicate zinc rich paint and optimum dimensions.

Component	Unit price [€]	Amount	Total Price [€]
Bolt (M30x110 S10T)	5.45	588	3205
		Total:	**3205**

Table 14. Material costs for friction connection 2 with ethyl silicate zinc rich paint and optimum dimensions.

Component	Unit price [€]	Amount	Total Price [€]
Bolt (M30x110 S10T)	5.45	351	1913
		Total:	**1913**

From these rough estimations, it appears that the material costs for the intermediate connections can be cut down by about 80%. The savings are here more than 20000€ per tower.

When possible, using weathering steel would decrease the required amount of bolts by about 40%. The additional costs for the steel plates could be compensated by the absence of coating.

Connections designed with resistances equivalent to the cross section yield strength would require more bolts and cost between 50% and 70% more.

However, it would still be about 70% cheaper than an equivalent flange connection.

The fabrication costs are not included in this estimation. However it is reasonable to think that, in serial production, they would be lower with friction connections.

The machining and drilling operations on one flange require around five hours. In an American study [21] this operation was estimated to cost about 3000$ per piece. The flanges must then be welded and if tolerances are not met, additional machining is required.

On the other hand the friction connections only require cutting the holes in the plates. This could be done by lasers before rolling. To avoid distortion the slots could be cut as closed and opened afterwards by cutting the tubes manually.

Another drawback of the flange connections which may be taken into account is the long delivery time, typically between three and four months.

The installation costs should also be considered. Although the friction connections require about four times as many bolts these are smaller and the tightening tools are easier to handle. The tightening procedure of Tension Control Bolts is also an advantage; *TCB Ltd.* reports tightening two times faster than with conventional bolts and only one operator is needed. From personal experience it took about two minutes to fully tighten a three bolts connection in two steps, including driving the nuts by hand. By extrapolation the tightening of friction connection 1 would require less than seven man hours. Also the wrenches from *TCB Ltd.* are electrical devices. They do not rely on hydraulic pressure which is time consuming and laborious to provide.

8.2.5 Final remarks on the costs assessment

The "HISTWIN" friction connection shifts the design limitations to other aspects of the tower and thus enable higher efficiency of the structure.

Used with the current tower geometry and material the cost analysis highlighted potential savings of about 80%, i.e. more than 20000€. Further savings are rather possible, based on the implementation of the "HISTWIN" friction connection.

The fatigue behaviour and effect on stability will be further studied to improve design and ensure its safety. In the same time the fabrication and in-situ assembling processes will be analyzed in co-operation with the producer of the steel tower involved in the project.

9 Door opening*)

9.1 Finite element analysis of the door opening

The commercially available software package ABAQUS, which is based on Finite Element Method, is used in analysis of the lower segment of the tower for wind turbine. The first seven meters of the REpower MM92 tower were modelled. The top of the door opening is at high of 3,65m and the next section available in the design load tables is the section in a height of 6,99m. This results in a distance between top of the door and top section of 3,34m.

The basic material properties used in the Finite Element Analysis (FEA) are shown in Table 15.

Table 15. *Material properties*

E-modulus	2,1 GPa
Poisson's ratio	0,3
Yield stress S 360	361 MPa
Yield strength S 690	690 MPa
Density	7850 kg/m³

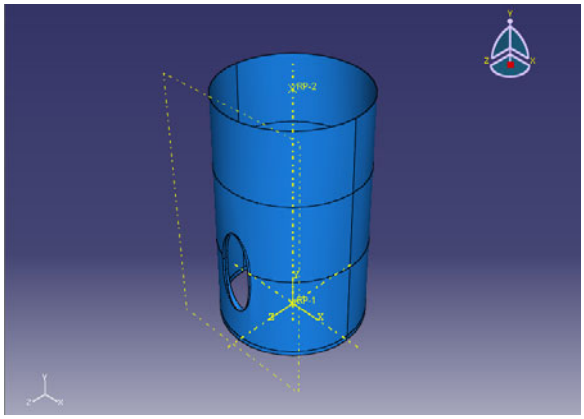

Figure 9-1. Lower tower section with FE mesh

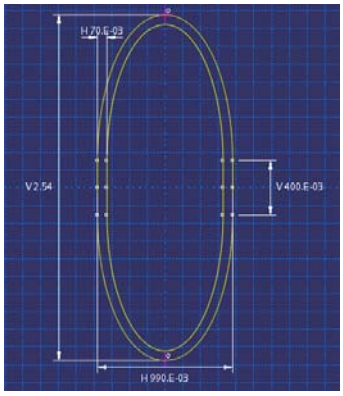

Figure 9-2. Geometry of the opening

The shell of the tower is divided into four sections; the bottom flange and the three sections of the lower part of the tower. The door is represented as a separate part and through a tie constraint added to the lower tower section. The geometric properties of the lower tower section used in the model are shown in Table 16.

*) The work presented in this chapter is based on on-going diploma work of Stefan Golling

Table 16. *Section properties*

Section name	Diameter at bottom [m]	Radius at bottom [m]	Section height [m]	Shell thickness [m]
Bottom Flange	4,3000	2,1500	0,15	0,030
Section 1	4,3000	2,1500	2,43	0,030
Section 2	4,2570	2,1285	2,33	0,030
Section 3	4,2150	2,1075	2,08	0,026

Section name (calculated values)	Diameter at top [m]	Radius at top [m]	Section height [m]	Shell thickness [m]
Section 3	4,1735	2,0868	2,08	0,026

Geometric imperfections are necessary to be considered in a model for a nonlinear analysis.

An imperfection based on eigen-value analysis and the shape of the critical buckling mode is the most usual way to assume initial imperfections. The critical bulking mode is obtained from buckling analysis. The maximum amplitude of it is displacement field has the maximum value 1.0. This displacement filed is normalised by the value of the maximum imperfection (an imperfection scaling factor). The maximum imperfection is allocated to node 733 which is just above the door opening.

9.2 FE mesh of the lower tower segment

The FE model consists of quadrilateral elements shell elements, S8R; which is an 8-node doubly curved shell with reduced integration. This element is used for stress/displacement analyzes were moments may be applied.

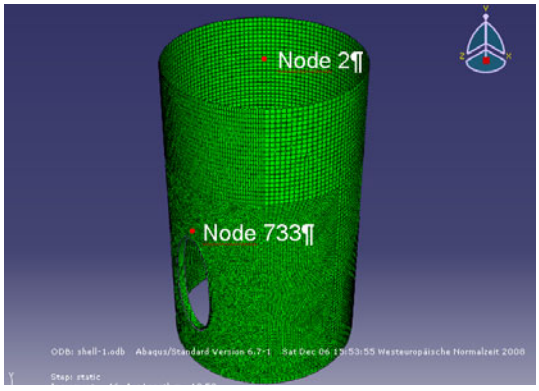

Figure 9-3. Lower tower section with mesh and "special" nodes used in FEA

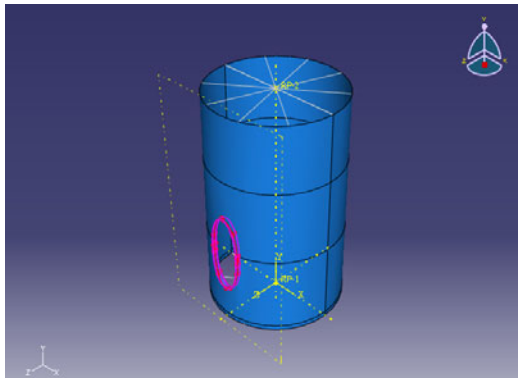

Figure 9-4. Tie and coupling constrain in the model

9.3 Parametric study of the stiffener and shell thickness

Following variables are varied in this analysis:

- the shell thickness of both sections considers, in a proportional way;
- the stiffener of the door opening thickness just for the shell thickness used in the tower MM92;
- the imperfection of the shell.

Table 17. Section properties

Model	Shell thickness Section 1 and 2 [m]	Shell thickness Section 3 [m]	Stiffener thickness [m]
Shell 1	0,030	0,026	0,070
Shell 2	0,020	0,017	0,070
Shell 3	0,015	0,013	0,070
Stiffener 2	0,030	0,026	0,050
Stiffener 3	0,030	0,026	0,030

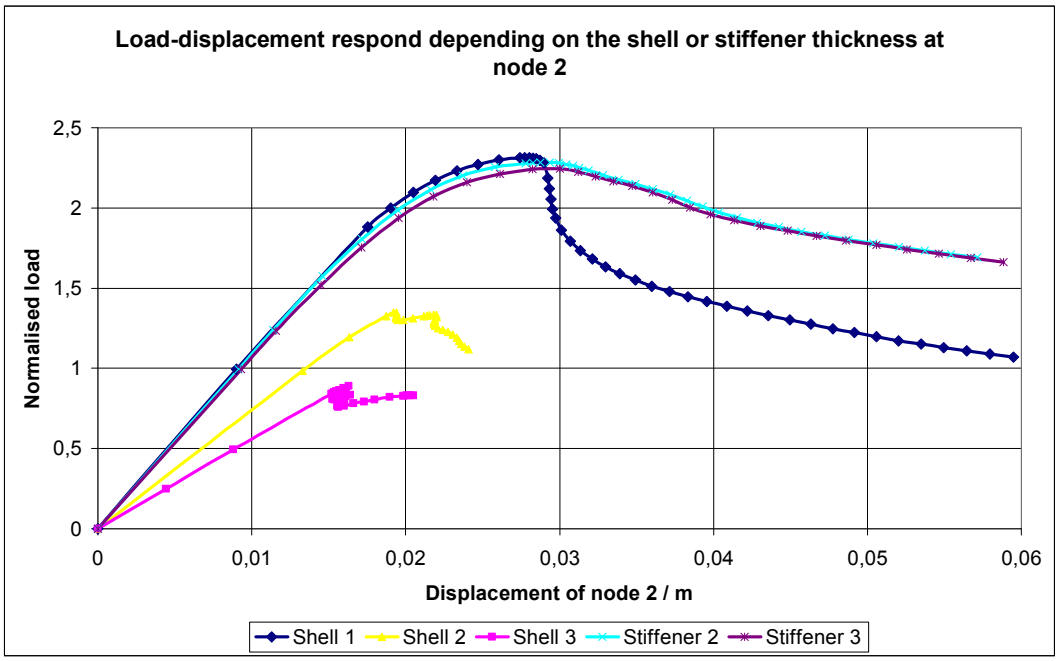

Figure 9-5 Load-displacement for various shell and stiffener thickness, the model without imperfections

The global behaviour of the tower without imperfections clearly leads to following conclusions:

- the reduce stiffener thickness does not effect the ultimate behaviour of the tower;

- with the reduced stiffener thickness concentration of stress increases to about 380 MPa for 30% reduction in thickness
- the 30% reduction of the tower thickness leads to the unsafe design if the S355 material used.

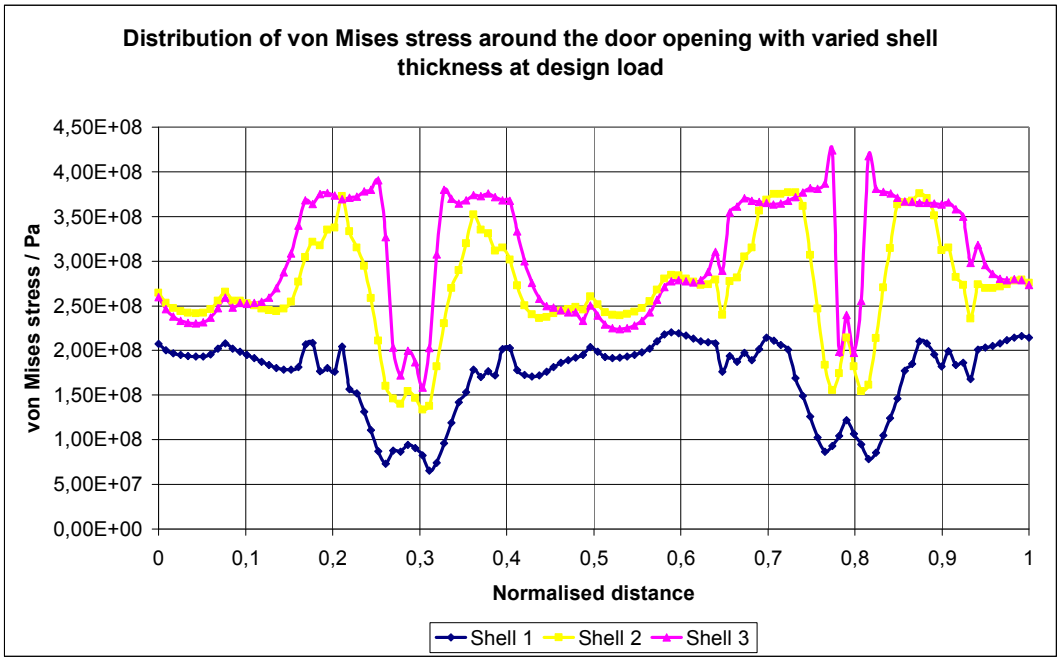

Figure 9-6. Stress distribution around the door opening for different shell thickness.

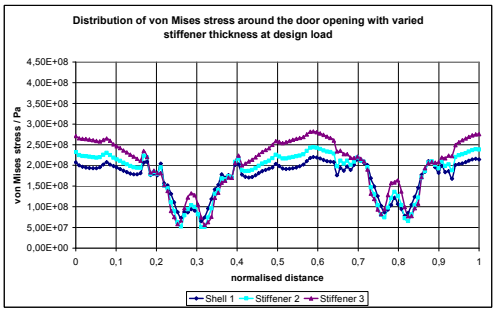

Figure 9-7. Stress distribution around the door opening for various stiffener thickness at design load.

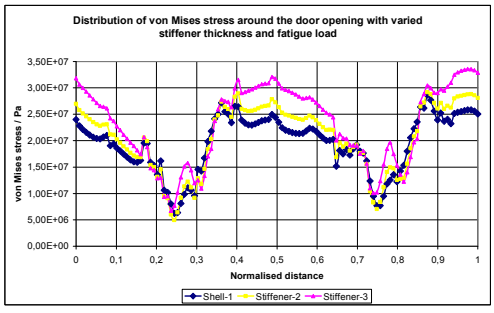

Figure 9-8. Stress distribution around the door opening for different stiffener thickness and at the fatigue design load

The results from these diagrams are self-explanatory.
If the level of imperfections is varied

Table 18. Geometrical properties for the parametric study

Name of the simulation used in following graphs	Imperfection value chosen for node 733 [m]	Imperfection value in percent of the shell thickness at node 733 [%]	Imperfection value introduced into the model [m]	Imperfection value in percent of the shell thickness at node with maximum amplitude [%]
Imp 0	0	0	0	0
Imp 1	0,003	10,0	0,0171	57
Imp 2	0,006	20,0	0,0342	114
Imp 3	0,016	53,7	0,0918	306

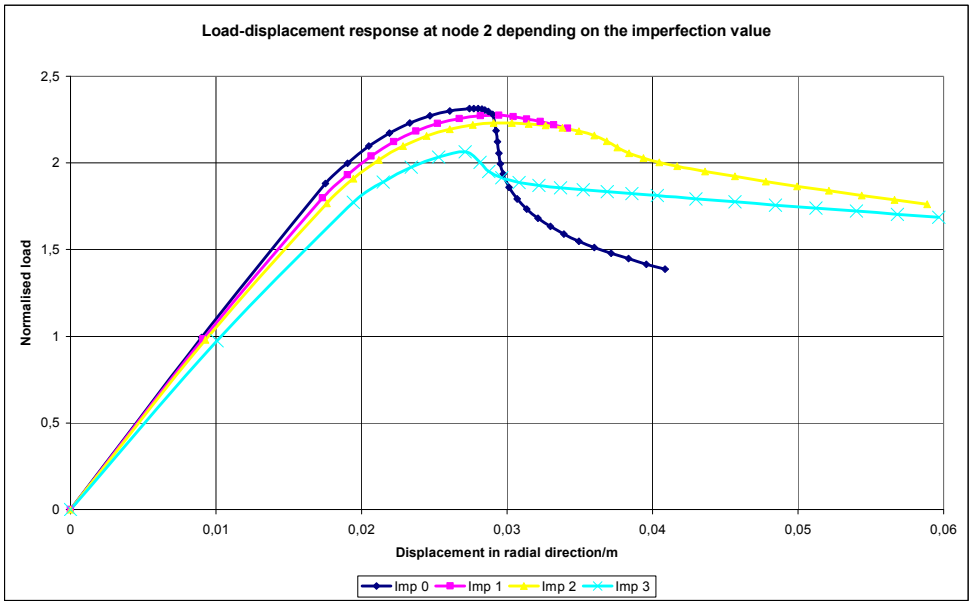

Figure 9-9 Load displacement of node 2, response depends on the value of initial imperfections

Figure 9-6 shows that the stiffness of the structure and the maximum load is decreasing with increasing initial imperfection. The value of "Imp 3" corresponds to Class 3 tolerance (normal) from Eurocode 3. The drop of the maximum load is about 12 % for the imperfections Class 3. It should be note that the used imperfection pattern is theoretical and no other imperfection, are taken into account.
The values of the Mises stress over the normalised distance of the door circumference are plotted in Figure 9-10. The maximum stress at the door opening with the highest imperfection shows that local yield may occur. This may indicates that the chosen imperfection value may be a bit too high.

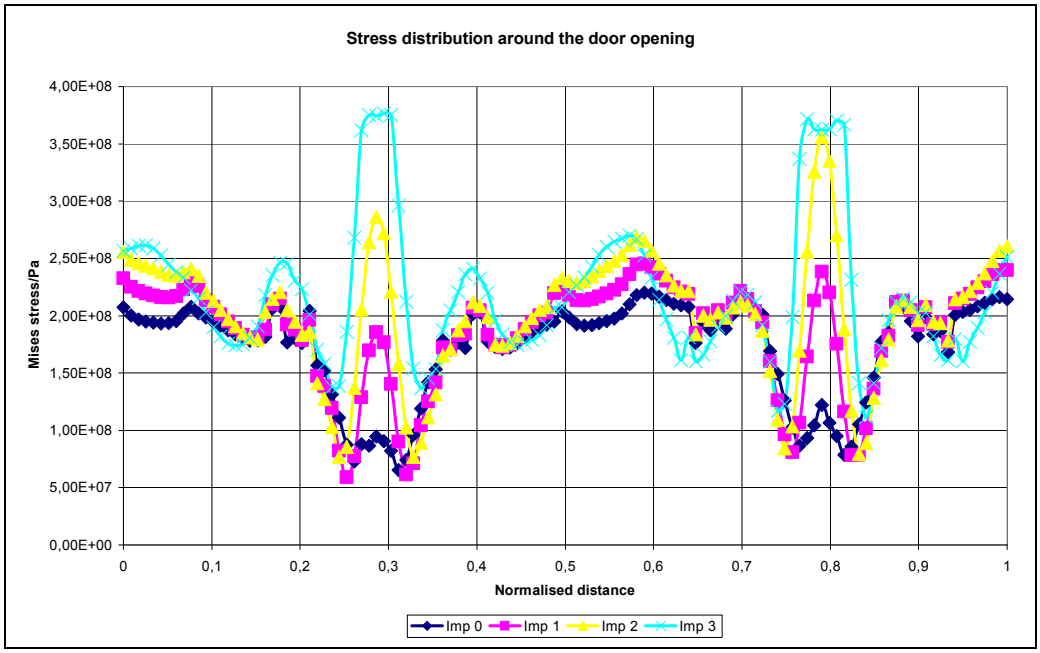

Figure 9-10 Normalised stress distribution around the door opening at the maximum load

9.4 A short parametric study with a high strength steel

Model shell 1, used in this chapter, is the tower MM92.
The initial imperfection value was 20% of the respective shell thickness of section one and two are introduced into the model. The basic model properties are shown in Table 19.

Table 19 Properties of the simulation models

	Yield strength	Shell thick. t_1 in Sec. 1 and 2	Shell thick. t_2 in Sect. 3	Stiff. thick.	Imperf. ampl. δ	δ/t_1
	[MPa]	[m]	[m]	[m]	[m]	
Shell 1	360	0,030	0,026	0,070	0,006	0,2
Shell 2	690	0,020	0,017	0,070	0,004	0,2
Shell 3	690	0,015	0,013	0,070	0,003	0,2
Shell 4	690	0,030	0,026	0,070	0,006	0,2
Shell 5	690	0,030	0,026	0,070	0,030	1,0
Shell 6	690	0,030	0,026	0,070	0,060	2,0

Results of this analysis are shown below.

The ultimate load for both models with high strength steel, "Shell 5" and "Shell 4" are around 47% or 57%, respectively, higher than the value of the original tower. The reduction of the ultimate load between the models with high strength steel is about 9% and increasing the initial imperfections amplitude by the factor 5. The stress distribution around the door opening is as a logical consequence lower than in the original model. The distribution around the door opening has a similar pattern as it was also visible and previous stress distributions. Model shell 5 shows the influence of increasing imperfection amplitudes on the stress distribution around the door. With increasing imperfection becomes the stress on top and at the bottom of the opening higher, to see at the normalised distance 0,28 and 0,78. At model shell 5 has the stress at this point already higher value than in the original structure.

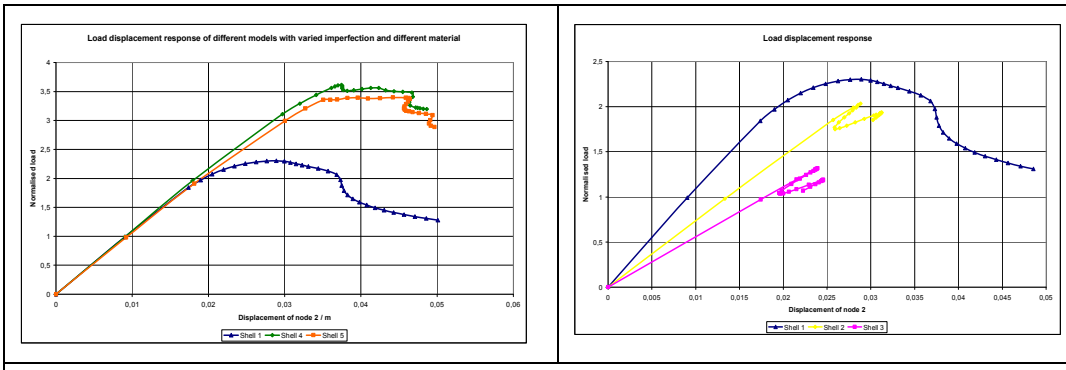

Figure 9-11. Load displacement response of the original tower and the tower with high strength steel and varied imperfection

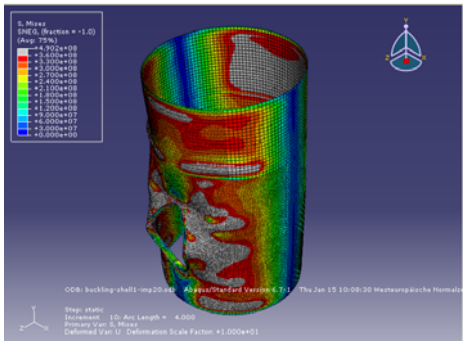

Figure 9-12. Model shell 1 at ultimate load

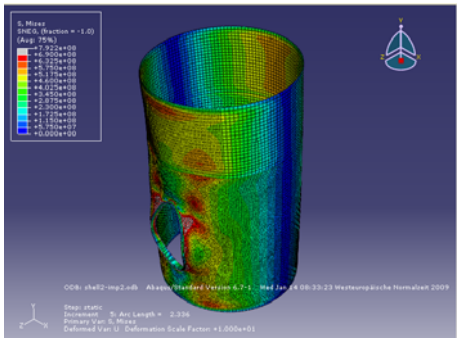

Figure 9-13 Model shell 2 at ultimate load

The results above indicate possibilities for use of higher strength steels. However more FEA results are necessary to quantify the above statement

References

[1] M. Seidel. Zur Bemessung geschraubter Ringflanschverbindungen von Windenergieanlagen. Universität Hannover, Institut für Stahlbau. 2001.

[2] Guideline for the certification of Wind Turbines, *Germanischer Lloyd WindEnergie*, Edition 2003 with Supplement 2004.

[3] M.S.G. Cullimore: Fatigue of HSFG Bolted Joints – Effects of Design Parameters. *Proceedings of the IABSE colloquium "Fatigue of Steel and Concrete Structures", International Assoc. for Bridge and Structural Engineering*, 1982.

[4] EN 1993-1-9 (2004). "*Eurocode 3 - Design of steel structures - Part 1-9: Fatigue*", CEN, European Committee for standardization, Brussels, Belgium.

[5] Joachim Dehm: 160-m-Fachwerkturm für eine Windenergieanlage - Die höchste Windenergieanlage der Welt. *Stahlbau*, Vol. 76, Heft 4, 2007, pp. 213-221.

[6] Meshulam Groper: Microslip and Macroslip. *Experimental Mechanics*, Vol.25, Nr.2, June 1985, pp. 171-174.

[7] Z. Shoukry W.H.: Bolted Connections with Varied Hole Diameters. *Journal of the Structural Division, ASCE*, Vol.96, ST6, June 1970, pp. 1105-1118.

[8] R.N. Allan and J.W. Fisher: Bolted Joints with Oversize or Slotted Holes. *Journal of the Structural Division, ASCE*, Vol.94, ST9, September 1968, pp. 2061-2080.

[9] G.L. Kulak; J.W. Fisher; J.H.A Struik: Guide to Design Criteria for Bolted and Riveted Joints. *AISC, Research Council on Structural Connections*, 2001, .

[10] Tension Control Bolts Limited, Whitchurch Business Park, Shakespeare Way, Whitchurch. Shropshire, SY13 1LJ England. www.tcbolts.co.uk, *Last visit: 2008-09-29*.

[11] T C Cosgrove: Tension Control Bolts, Grade S10T, in Friction Grip Connections. *The Steel Construction Institute*, 2004.

[12] I. Ryan: Evaluation of the high strength "bolt for pre-loading" product type "TCB" and its use in France. *Centre Technique Industriel de la Construction Metallique, CTICM N°2001-07*, October 2001.

[13] SS-EN ISO 8501-1 (2007). "*Preparation of steel substrates before application of paints and related products - Visual assessment of surface cleanliness - Part 1: Rust grades and preparation grades of uncoated steel substrates and of steel substrates after overall removal of previous coatings*", Swedish Standards Institute, Stockholm, Sweden.

[14] A. Panait. Étude expérimentale et numérique des problèmes de contact unilatéral et de frottement sec dans les assemblages verriers. Université de Marne la Vallée. juin 2004.

[15] EN 1993-1-8 (2005). "*Eurocode 3 - Design of steel structures - Part 1-8: Design of joints*", CEN, European Committee for standardization, Brussels, Belgium.

[16] prEN 1090-2 (2007). "*Execution of steel structures and aluminium structures – Part 2: Technical requirements for the execution of steel structures — Stage 49R*", CEN, European Committee for standardization, Brussels, Belgium.

[17] M.B. Marshall; R. Lewis; R.S. Dwyer-Joyce: Characterisation of Contact Pressure Distribution in Bolted Joints. *Strain*, Vol. 42, 2006, pp. 31-43.

[18] T. Siwowsk; Z. Manko: The fatigue strength of HSFG Bolted Joints in steel bridges. *Swedish Institute of Steel Construction, Proceedings of Nordic Steel Construction Conference' 95, Sweden, Volume I*, 1995.

[19] EN 1990 (2002). "*Eurocode - Basis of structural design*", CEN, European Committee for standardization, Brussels, Belgium.

[20] W. Husson. Friction connections with slotted holes for wind towers. Luleå University of Technology. 2008:45.

[21] N.W. LaNier: LWST Phase I Project Conceptual Design Study: Evaluation of Design and Construction Approaches for Economical Hybrid Steel/Concrete Wind Turbine Towers. *National Renewable Energy Laboratory, NREL/SR-500-36777*, January 2005.

Annex 1-Publications and conferences in 2008

List of publications in 2008

A. Hammer Jeppesen: An alternative connection in steel towers for wind turbines. Luleå University of Technology, September 2008.

W. Husson: Friction Connections with Slotted Holes for Wind Towers. Licentiate thesis 2008:45, December 2008.

List of conferences and workshops in 2008

W. Husson; M. Veljkovic: Safe and Innovative Connection in Tubular Steel Towers for Wind Turbines. EWEC 2008, 31 March -3 April 2008, Brussels, Belgium.

M. Veljkovic: Höghållfasta torn, Forskning om vindkraft i fokus, Vindforsk programkonferens 14-15 maj, Stockholm

W. Husson; M. Veljkovic: Performance of a High Strength Friction Grip Connection with Open Slotted Hole. International Workshop on Connections in Steel Structures: Connections VI, Chicago, USA, 23-25 June 2008.

W. Husson; M. Veljkovic: Innovative connection in tubular steel towers – Experiments on segment specimens under static loading. EUROSTEEL 2008, Graz, Austria, 3-5 September 2008.

M. Veljkovic: Ny typ av ståltorn för framtida vindturbiner med höga torn och höga effekter, Elforskdagen, oktobar 14, 2008, Stockholm

W. Husson; M. Veljkovic: Resistance of Friction Connections with long slotted holes. International seminar and open workshop – New connection detailing of towers for wind turbines, Hamburg, Germany, 5 November 2008.